A Selective Prostaglandin E 2 Receptor Subtype 2 (EP2) Antagonist Increases the Macrophage-Mediated Clearance of Amyloid-Beta Plaques

14 AUTHORS, INCLUDING:

Frank Kayser

46 PUBLICATIONS **1,105** CITATIONS

SEE PROFILE

Hannah Dou

Amgen

5 PUBLICATIONS **118** CITATIONS

SEE PROFILE

Toni L. Williamson

Flexion Therapeutics

29 PUBLICATIONS **1,183** CITATIONS

SEE PROFILE

Ji Ma

Amgen

23 PUBLICATIONS **258** CITATIONS

SEE PROFILE

A Selective Prostaglandin E₂ Receptor Subtype 2 (EP2) Antagonist Increases the Macrophage-Mediated Clearance of Amyloid-Beta Plaques

Brian M. Fox,*,[†] Hilary P. Beck,[†] Philip M. Roveto,[†] Frank Kayser,[†] Qingwen Cheng,[†] Hannah Dou,[†] Toni Williamson,[‡] James Treanor,[†] Hantao Liu,[‡] Lixia Jin,[†] Guifen Xu,[†] Ji Ma,[†] Songli Wang,[†] and Steven H. Olson[†]

[†]Amgen South San Francisco, Amgen Inc., 1120 Veterans Boulevard, South San Francisco, California 94080, United States
[‡]Amgen Inc., One Amgen Center Drive, Thousand Oaks, California 91320, United States

Ⓢ Supporting Information

ABSTRACT: A high-throughput screen resulted in the discovery of benzoxazepine **1**, an EP2 antagonist possessing low microsomal stability and potent CYP3A4 inhibition. Modular optimization of lead compound **1** resulted in the discovery of benzoxazepine **52**, a molecule with single-digit nM binding affinity for the EP2 receptor and significantly improved microsomal stability. It was devoid of CYP inhibition and was ~4000-fold selective against the other EP receptors. Compound **52** was

EP2 selective antagonist increases Aβ phagocytosis

shown to have good PK properties in CD-1 mice and high CNS permeability in C57Bl/6s mice and Sprague−Dawley rats. In an ex vivo assay, it demonstrated the ability to increase the macrophage-mediated clearance of amyloid-beta plaques from brain slices in a dose-dependent manner.
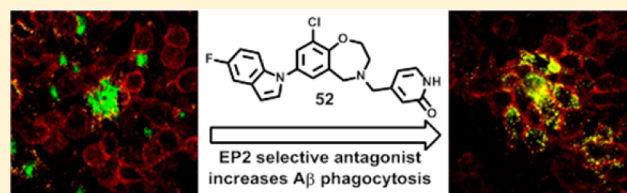
■ INTRODUCTION

Alzheimer's disease (AD) is characterized by the accumulation of amyloid-beta (Aβ) plaques, neurofibrillary tangles, and neurodegeneration.[1] Although the exact cause of neurodegeneration is still under debate, it is likely that Aβ plaques contribute because aggregated Aβ is directly toxic to neurons.[2,3] Several lines of evidence indicate that microglia are responsible for the clearance of Aβ plaques in the CNS. Microglia surround and infiltrate Aβ plaques in human and mouse brain.[4−11] Microglia clear Aβ plaques by phagocytosis,[2,4,12−14] and activation of microglia by Aβ immunization or LPS exposure causes an increase in microglial-mediated phagocytosis.[11,13,15] While clearance of Aβ plaques should be beneficial, exposure of microglia to Aβ plaques elicits an innate immune response that causes the release of proinflammatory cytokines such as IL-1β, IL-6, tumor necrosis factor α (TNFα), the chemokines IL-8, MIP-1α, and MCP-1, the growth factor (M-CSF), along with glutamate, complement proteins, peroxynitrite, and superoxide radicals.[16−19] This potent inflammatory response results in oxidative damage and neurotoxicity.

Recent evidence indicates that although microglia are beneficial in clearing plaques at the onset of AD, they become dysfunctional and lose their ability to clear plaques as the disease progresses. Chronic exposure of microglia to aggregated Aβ in mice results in the reduced expression of Aβ-binding receptors and Aβ-degrading enzymes, resulting in a reduction in their ability to clear plaques by phagocytosis.[20,21] While there is a reduction in the ability to clear plaques, the microglia continue to produce a robust neurotoxic inflammatory response.

A similar phenotype has been demonstrated in AD patients where microglia lose their ability to clear Aβ plaques and develop a consistent proinflammatory response.[22,23] Thus, it has been hypothesized that microglia are unable to clear, through phagocytosis, the significant amount of aggregated Aβ present in the brains of AD patients. This results in a chronic Aβ-stimulated microglial-mediated inflammatory response that causes neurotoxicity and exacerbates the disease pathology.[20,21,24]

Although many factors may play a role in the accumulation of Aβ in Alzheimer's disease, several lines of evidence indicate that prostaglandin E₂ (PGE₂) is a key contributor. PGE₂ dose-dependently inhibits macrophage-mediated phagocytosis,[25] and elevated levels of PGE₂ have been observed in the brains of patients with AD.[26] PGE₂ is the natural ligand of four prostanoid receptors, termed prostaglandin E₂ receptor subtypes 1−4 (EP1, EP2, EP3, and EP4).[27] Several lines of evidence indicate that PGE₂ inhibits the microglial-mediated phagocytosis of aggregated Aβ through the EP2 receptor. Microglia from mice lacking the EP2 receptor (EP2−/−) have significantly increased phagocytosis of aggregated Aβ compared to wild-type (wt) microglia in vitro.[3] Microglia lacking EP2 also demonstrated enhanced phagocytosis of Aβ plaques present on hippocampal sections from patients who died with Alzheimer's disease.[3] Deletion of the EP2 receptor in the APPSwe-PS1ΔE9 mouse model of familial Alzheimer's disease resulted in a significant reduction of Aβ plaques and Aβ40 and Aβ42 levels compared

to mice possessing the EP2 receptor.[28] The decrease in Aβ was shown to be mediated by microglia by demonstrating that APPSwe-PS1ΔE9 mice that were irradiated and then implanted with bone marrow from EP2−/− mice had reduced Aβ levels compared to mice implanted with bone marrow from wt mice.[29]

In addition to playing a role in Aβ phagocytosis, the EP2 receptor is required to elicit the microglial-mediated innate immune response. Deletion of EP2 significantly reduces inflammation and the resulting oxidative damage after a LPS challenge.[28,30,31] Exposure of neurons to LPS causes neurotoxicity as a result of the microglial-mediated activation of innate immunity that is EP2 dependent.[32] In a similar manner, incubation of primary neurons with aggregated Aβ causes neurotoxicity that is exacerbated by the presence of wt microglia. In contrast, incubation of primary neurons with aggregated Aβ in the presence of EP2−/− microglia caused no neurotoxicity.[3] While this data clearly implicated the involvement of the EP2 receptor in the phagocytosis of Aβ plaques and the resulting neurotoxic inflammatory response, the role of EP2 in the development of Alzheimer's disease remained unclear. Recent evidence demonstrated that aging or Aβ accumulation caused the upregulation of microglial EP2 signaling. This increased proinflammatory gene expression and suppressed beneficial chemokine production and chemotaxis, resulting in a reduction in Aβ clearance.[33] This data may explain why microglia become dysfunctional in patients with AD and are unable to clear accumulating Aβ plaques.

The EP2 receptor has been implicated in the etiology of several neurodegenerative diseases in addition to Alzheimer's disease, including Parkinson's disease (PD), amyotrophic lateral sclerosis (ALS), and epilepsy.[34] Furthermore, deletion of the EP2 receptor has demonstrated beneficial effects in mouse models of AD, PD, and ALS.[34] For many years, the lack of selective tool molecules have made it difficult to further interrogate the role of the EP2 receptor in these neurodegenerative diseases, however, recent reports describe the discovery of selective EP2 antagonists,[35−41] including the demonstration that they reduce brain inflammation and neuronal injury in a mouse model of status epilepticus.[37,38]

Consideration of the data discussed above indicates that inhibiting the activation of the microglial EP2 receptor with a small molecule antagonist provides an extremely attractive approach to treating AD by increasing the phagocytosis of neurotoxic Aβ plaques while at the same time abrogating the neurotoxic inflammatory response caused when microglia are exposed to aggregated Aβ.

■ RESULTS AND DISCUSSION

A high-throughput screen of our small molecule library resulted in the discovery of benzoxazepine 1 as a novel EP2 antagonist with moderate potency across the human, rat, and mouse receptors (Table 1). Compound 1 was greater than 400-fold selective over the EP1 receptor, 300-fold selective over the EP3 receptor, and 50-fold selective against the EP4 receptor. Benzoxazepine 1 was a potent inhibitor of both CYP3A4 and 2D6 and had low microsomal stability in human and rat liver microsomes. Despite these issues, we considered compound 1 to be a good starting point for lead optimization due in part to the low MW (402.5 g/mol), low PSA (34.5 Å^2), absence of H-bond donors, and reasonable cLogD$_{7.4}$ (5.3) that should provide 1, and compounds of similar structure, appreciable CNS permeability.

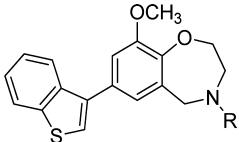**Table 1. Potency, Selectivity, and in Vitro ADME Data for 1**

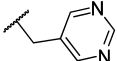| EP2 Potency[a]	
hEP2 SPA IC$_{50}$: 0.07 ± 0.04 μM	hEP2 cAMP IC$_{50}$: 0.6 ± 0.4 μM
rEP2 SPA IC$_{50}$: 0.1 ± 0.05 μM	rEP2 cAMP IC$_{50}$: 0.3 ± 0.2 μM
mEP2 SPA IC$_{50}$: 0.1 ± 0.03 μM	mEP2 cAMP IC$_{50}$: 0.06 ± 0.03 μM
Selectivity[a]	
hEP1 SPA IC$_{50}$: >30 μM	hEP3 SPA IC$_{50}$: 23 ± 10 μM
hEP4 SPA IC$_{50}$: 3.5 ± 1.6 μM	
In Vitro ADME	
CYP3A4$_{inh}$ @ 3 μM = 97%	CYP2D6$_{inh}$ @ 3 μM = 48%
HLM CL: >399 μL/min·mg	RLM CL: >399 μL/min·mg
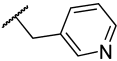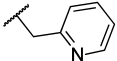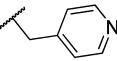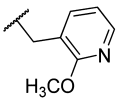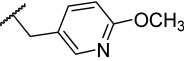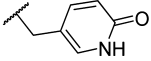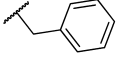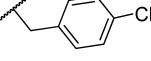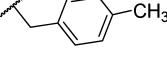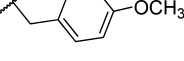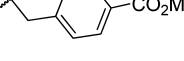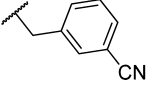
[a]Data are reported as the average of a minimum of two determinations.
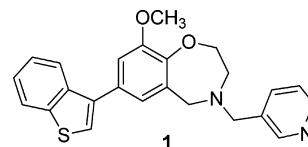
Lead compound 1 was separated into fragments consisting of the benzothiophene ring, pyridine ring, and benzoxazepine core, and each was optimized independently. The potent inhibition of CYP3A4 and 2D6 by 1 is of concern because these two isoforms metabolize more than 50% of clinically important drugs; therefore, inhibition of either of these isoforms has the potential to cause significant drug−drug interactions in patients receiving more than one drug substance.[42] The pyridine ring was suspected to be responsible for the potent CYP inhibition observed for benzoxazepine 1 due to the well-documented ability of pyridine nitrogens to interact with the iron in the heme-containing CYP enzymes.[43] The inhibition of CYP enzymes by pyridines can be mitigated by the introduction of steric encumberance around the pyridine nitrogen or by reducing the basicity of the pyridine nitrogen.[43] Moving the pyridyl nitrogen to the 2-position resulted in a significant decrease in the inhibition of both CYP3A4 and 2D6, likely due to the increased steric bulk around the pyridyl nitrogen (Table 2). Unfortunately, this also resulted in a 10-fold decrease in EP2 potency. The 4-pyridyl analogue 3 had similar CYP inhibition values compared to 1 and resulted in a 3-fold loss in EP2 potency. Reducing the basicity of the pyridine nitrogen by replacement with pyrimidine 4 resulted in an increase in EP2 potency but no improvement in CYP3A4 inhibition. On the basis of these results, molecules were prepared that had both decreased basicity and increased steric bulk around the pyridine nitrogen. This provided methoxy pyridines 5 and 6 and pyridone 7 that were very successful in reducing the CYP3A4 inhibition while retaining EP2 potency.

The second approach investigated to reduce the CYP inhibition was to remove the pyridine nitrogen altogether. Converting the pyridine ring to a phenyl ring provided analogue 8 that was devoid 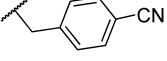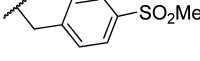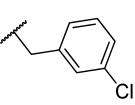of CYP3A4 inhibition but had significantly reduced EP2 potency. Variation of substituents on the phenyl ring revealed that hydrophobic groups were not tolerated (chloro and methyl analogues 9, 10, and 15). In contrast, placing H-bond acceptors at the 3- and 4-positions provided compounds 11−14 and 16 that possessed increased EP2 potency compared to phenyl analogue 8. Two of the most potent phenyl analogues prepared were sulfone 14 and nitrile 16, each being 100-fold more potent than phenyl analogue 8. In addition, they possessed significantly reduced CYP inhibition

Table 2. hEP2 IC$_{50}$ Values and CYP Inhibition Data for Compounds 1−16

Compound	R	hEP2 SPA IC$_{50}$ (μM)[a]	hEP2 cAMP IC$_{50}$ (μM)[a]	% inhibition CYP3A4 @ 3 μM	% inhibition CYP2D6 @ 3 μM
1	(3-pyridylmethyl)	0.07 ± 0.04	0.6 ± 0.4	97	48
2	(2-pyridylmethyl)	0.7 ± 0.3	3.0	39	19
3	(4-pyridylmethyl)	0.2 ± 0.03	0.9 ± 0.4	89	93
4	(pyrimidinylmethyl)	0.02 ± 0.01	0.08 ± 0.02	93	29
5	(2-methoxy-3-pyridylmethyl)	0.2 ± 0.07	1.1	28	83
6	(6-methoxy-3-pyridylmethyl)	0.1 ± 0.02	1.5	21	40
7	(2-oxo-pyridinylmethyl)	0.2 ± 0.05	0.5 ± 0.08	<10	37
8	(benzyl)	10	>30	13	69
9	(4-chlorobenzyl)	30	>30	10	40
10	(4-methylbenzyl)	30	>30	14	73
11	(4-methoxybenzyl)	1.8	>30	23	50
12	(4-CO$_2$Me-benzyl)	0.6 ± 0.2	>30	<10	<10
13	(4-CN-benzyl)	0.6 ± 0.1	>30	13	<10
14	(4-SO$_2$Me-benzyl)	0.1 ± 0.05	NT	<10	13
15	(3-chlorobenzyl)	30	NT	24	57
16	(3-CN-benzyl)	0.1 ± 0.02	1.0	32	28

[a]Data with SD are reported as the average of a minimum of two determinations.

values compared to lead compound **1** while having similar EP2 IC$_{50}$ values. Investigating analogues of the pyridine ring revealed that the pyridine nitrogen was responsible for CYP3A4 inhibition and that H-bond acceptors greatly

improved EP2 potency. While the SAR trend for the inhibition of CYP2D6 was less straightforward, several replacements of the pyridine ring, such as the pyridone ring in **7** and the 4-methylsulfonylphenyl ring in **14**, provided analogues that possessed similar EP2 potency compared to **1** while also significantly decreasing CYP3A4 and CYP2D6 inhibition.

Incubation of lead compound **1** with liver microsomes revealed that multiple oxidative metabolites were formed at several positions of this molecule. This included several oxidative metabolites of the benzothiopene ring of **1**, therefore, replacement of this ring was a high priority. Initial work indicated that maintaining a hydrophobic group in the area occupied by the benzothiophene phenyl ring was crucial to maintaining EP2 potency. For example, removing the phenyl ring to provide thiophene **17** resulted in complete loss of EP2 potency while altering the position of the phenyl ring to the 2-linked benzothiopene **18** resulted in a compound with micromolar potency (Table 3). The importance of the phenyl ring was also demonstrated by the significant increase in potency of naphthalene **20** compared to phenyl analogue **19**. Attempts to replace the second phenyl ring of naphthalene analogue **20** with monosubstituted phenyl analogues of **19** indicated that polar groups were not tolerated (data not shown). In contrast, *m*-methyl analogue **22** was equipotent to **19**, while the *o*- and *p*-methyl isomers **21** and **23** were devoid of EP2 activity. The meta position was also optimal for the chloro analogues with *m*-chloro derivative **25**, demonstrating a 20-fold increase in potency over **19** while the *o*- and *p*-chloro isomers **24** and **26** were equipotent to **19**. Despite the improved potency, *m*-chlorophenyl analogue **25** was still 10-fold less potent than compound **1**, which possessed a benzothiophene ring. This led to the conclusion that heterocyclic rings containing a phenyl ring in a similar position to the benzothiophene phenyl ring should be explored.

It quickly became clear that the SAR was very sensitive to thiophene replacements with increased polarity. Incorporation of a nitrogen atom to provide benzoisothiazole **27** resulted in a 6-fold loss in EP2 potency while increasing the polarity further by converting this ring to a benzimidazole **28** resulted in nearly a 10-fold loss in potency compared to compound **1**. Results obtained from 1-linked indole **29** and 3-linked indole analogues **30** and **31** further demonstrated that sulfur and carbon atoms were preferred at positions analogous to the 1- and 2-positions of the benzothiophene ring.

The 1-linked indole ring contained in **29** proved to be the most potent heterocyclic ring replacement for the benzothiophene in this series, but it was still more than 4-fold less potent than lead compound **1**. Earlier work investigating the SAR of phenyl analogue **19** demonstrated a strong preference for hydrophobic groups in this area of the binding pocket with a chlorine atom, providing the largest increase in EP2 potency. Therefore, in an attempt to increase the potency of the 1-linked indole series, several chloroindole isomers were prepared. Within this series, 3-chloroindole **32** and 5-chloroindole **34** had the highest EP2 binding affinity, with IC$_{50}$ values of 60 and 80 nM, respectively, while 4-, 6-, and 7-substituted indole analogues **33**, **35**, and **36** all had significantly higher IC$_{50}$ values. Furthermore, the 3-, 4-, and 6-chloroindole isomers **32**, **33**, and **35** were all shown to be weak partial agonists for the human EP2 receptor (data not shown). These data warranted further investigation of 5-substituted indole analogues. The 5-cyanoindole, 5-fluoroindole, and 5-chloroindoline compounds **37**, **38**, and **39** all demonstrated EP2 affinity in the

SPA assay that was comparable to **1**, while **38** and **39** also demonstrated a 10-fold increase in potency in the cAMP assay compared to benzothiophene **1**. The microsomal stability of each compound in Table 3 was similar to benzothiophene **1**. The lack of improvement in microsomal stability is not unexpected, as the metabolite identification of lead compound **1** indicated that metabolism occurred at several positions of this molecule. It is likely that reducing metabolism in a single section of this molecule will not result in a detectable difference in microsomal stability but will require several changes in the overall structure.

In addition to oxidation of the benzothiophene ring, metabolite identification indicated that the methoxy group on the benzoxazepine ring is readily demethylated when **1** is incubated with liver microsomes. Thus, it is likely that removal or replacement of the methoxy group would be required to provide a molecule with acceptable metabolic stability. Removing the methoxy group to provide **40** resulted in a 15-fold reduction in EP2 potency. The phenol metabolite **41** was also prepared and shown to be greater than 20-fold less active against the EP2 receptor. Increasing the size of the methyl ether to ethyl **42** and isopropyl **43** also resulted in a significant loss in potency. Replacement of the methyl ether with a methyl group provided analogue **44** that showed similar potency compared to **1**. Chlorine proved to be the optimal replacement of the methyl ether, providing compound **45** that was equipotent to **1** while at the same time removing a metabolic liability that contributed to the poor microsomal stability of the series. Not surprisingly, because of the multiple metabolic soft spots none of the compounds in Table 4 demonstrated an improvement in microsomal stability compared to methyl ether **1**.

Changes to the oxazepine ring were also investigated (Table 5). Replacing the oxygen atom of the oxazepine ring with a carbon atom provided a compound with similar potency (benzoazepine **46** vs benzoxazepine **40**), while replacement with a nitrogen atom resulted in a minimal loss in potency (**47** and **48** vs **40**). Both lactam analogues prepared (**49** and **50**) demonstrated low EP2 affinity.

The modular approach taken to investigate the SAR of benzoxazepine **1** resulted in several key discoveries. Replacement of the pyridine ring provided several compounds that retained EP2 potency and were devoid of CYP3A4 inhibition, including methoxy pyridines **5** and **6**, pyridone **7**, 3-cyanophenyl analogue **16**, and 4-methylsulfonylphenyl analogue **14**. Replacement of the benzothiophene ring with a 5-fluoroindole ring **38** or a 5-chloroindoline ring **39** provided analogues that were equipotent to **1** in the SPA assay and significantly more potent in the cAMP assay. It was discovered that replacement of the oxazepine oxygen atom with a carbon atom resulted in a compound with similar EP2 potency (**46** vs **40**). Furthermore, the methyl ether could be replaced with a chlorine atom with no loss in potency in the SPA assay and a minimal loss of activity in the cAMP assay. Because of the multiple sites of metabolism, no single change made during this modular approach resulted in an improvement in microsomal stability. However, it is likely that many of these changes have an impact on the microsomal turnover that is undetectable because the groups that remain are metabolically labile. In this case, it is predicted that the combination of several groups would provide a molecule with a detectable improvement in microsomal stability. In a similar manner, the combination of groups that provided modest increases in potency would be

Table 3. hEP2 IC$_{50}$ Values for Compounds 17−39

Compound	R	hEP2 SPA IC$_{50}$ (μM)[a]	hEP2 cAMP IC$_{50}$ (μM)[a]	Compound	R	hEP2 SPA IC$_{50}$ (μM)[a]	hEP2 cAMP IC$_{50}$ (μM)[a]
1		0.07 ± 0.04	0.6 ± 0.4	28		6.4	15
17		>30	>30	29		0.3 ± 0.1	1.0 ± 0.3
18		2.8	4.8	30		2.7	3
19		15	>30	31		1.1	2.5
20		0.3 ± 0.09	2.5	32		0.06 ± 0.02	0.9 ± 0.4
21		>30	>30	33		0.4 ± 0.1	3.3
22		15	13	34		0.08 ± 0.03	0.7 ± 0.2
23		>30	>30	35		0.8 ± 0.3	4
24		12	>30	36		5.6	>30
25		0.7 ± 0.2	1.9	37		0.1 ± 0.04	0.2 ± 0.05
26		10	>30	38		0.09 ± 0.04	0.04 ± 0.01
27		0.4 ± 0.05	0.6 ± 0.2	39		0.03 ± 0.02	0.06 ± 0.03
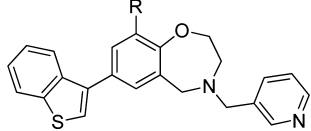
[a]Data with SD are reported as the average of a minimum of two determinations.

additive and provide compounds with significant increases in EP2 potency.

The results obtained from combining some of the best fragments are shown in Figure 1. As discussed earlier, replacement of the methyl ether of **1** with chlorine while retaining the benzothiophene and pyridine ring to provide **45** resulted in no improvement in microsomal stability. However, when the methyl ether to chlorine change was coupled with the

Table 4. hEP2 IC$_{50}$ Values for Compounds 40−45

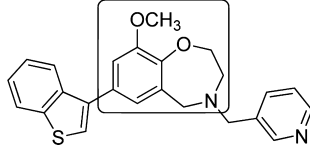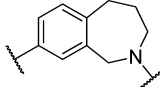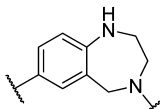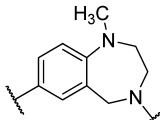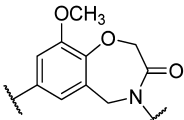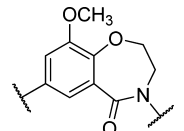| Compound	R	hEP2 SPA IC$_{50}$ (μM)[a]	hEP2 cAMP IC$_{50}$ (μM)
40	H	1.1	>30
41	OH	1.5	3.8
42	OEt	14	>30
43	Oi-Pr	>30	>30
44	CH$_3$	0.2 ± 0.06	1.0
45	Cl	0.08 ± 0.03	2.5

[a]Data with SD are reported as the average of a minimum of two determinations.

replacement of the pyridine ring by a pyridone ring, a significant improvement in microsomal stability was achieved (**51** vs **1** and **45**). Replacement of the benzothiophene ring in **51** with the 5-fluoroindole ring provided compound **52** that possessed similar microsomal stability compared to **51** and a significant increase in EP2 potency. Combination of the three optimal replacements of benzothiophene to 5-fluoroindole, methyl ether to chlorine, and pyridine to pyridone provided benzoxazepine **52** that was 10-fold more potent than **1** in the SPA and cAMP assays, was devoid of CYP inhibition, and possessed significantly increased microsomal stability compared to lead compound **1**.

Lead compound **1** displayed greater than 400-fold selectivity against the hEP1 receptor, 300-fold selectivity against the hEP3 receptor, and 50-fold selectivity against the hEP4 receptor. Signaling through the EP receptors has versatile and often opposing actions in many tissues.[27] All four EP receptors are expressed in the CNS including the expression of EP1 and EP2 on microglia.[44] Because of the presence of multiple EP receptors in the CNS and the wide array of physiological roles mediated by them, one of the objectives of this project was to increase the selectivity against the EP3 and EP4 receptors. This would ensure that any effects observed would be due to signaling through the EP2 receptor alone. Conversion of the methyl ether of benzoxazepine **1** to chloride **45** failed to provide any increase in selectivity (Figure 2). Combining this change with the conversion of the pyridine ring to a pyridone ring provided **51** that was 900-fold selective against the hEP4 receptor. Replacing the benzothiophene ring with a 5-fluoroindole ring (**52**) or adding a methyl group alpha to the oxazepine nitrogen (**53**) further increased the selectivity to ~4000-fold. Finally, combination of the four changes discussed above provided benzoxazepine **54** that was shown to have a 10000-fold higher binding affinity for the hEP2 receptor compared to the hEP4 receptor. While it required several changes in the structure of compound **1** to provide high selectivity against the hEP4 receptor, each of the compounds shown in Figure 2, with the exception of **1**, had hEP3 binding

Table 5. hEP2 IC$_{50}$ Values for Compounds 46−50

Compound	R	hEP2 SPA IC$_{50}$ (μM)	hEP2 cAMP IC$_{50}$ (μM)
46		1.6	>30
47		6	>30
48		4	>30
49		13	>30
50		>30	>30

affinity values greater than the highest tested concentration. The lack of binding affinity for the hEP1 receptor was also maintained for all of the compounds in this series.

Benzoxazepine **52** demonstrated comparable potency across the human, rat, and mouse EP2 receptors (Table 6). Compound **52** was further profiled against the human prostanoid receptors DP, TP, IP, and CRTH2. For each receptor, an aequorin assay was used to determine an IC$_{50}$ value of the antagonism of an agonist ligand, as well as an EC$_{50}$ value in the absence of an added agonist. Compound **52** was greater than 660-fold selective in the hEP2 cAMP assay versus all four receptors.

Benzoxazepine **52** had moderate clearance in CD-1 mice with a corresponding half-life of 3.4 h and good bioavailability and exposure when dosed orally (Table 7). The ability of compound **52** to access the CNS was measured in both C57BL/6s mice and Sprague−Dawley rats. Animals were dosed orally with **52** followed by sacrificing mice after 2 h and rats after 3 h. Concentrations measured in plasma and brain homogenate demonstrated that compound **52** had good CNS exposure in C57BL/6s and in Sprague−Dawley rats with brain/plasma ratios of 0.7 and 0.9, respectively.

The ability of benzoxazepine **52** to increase macrophage-mediated Aβ phagocytosis was studied using an ex vivo assay. Plaque-bearing brain slices from 18 month old Tg2576 mice[45] were incubated for 24 h in the presence of mouse peritoneal macrophage IC21 cells (ATCC TIB-186) and vehicle or
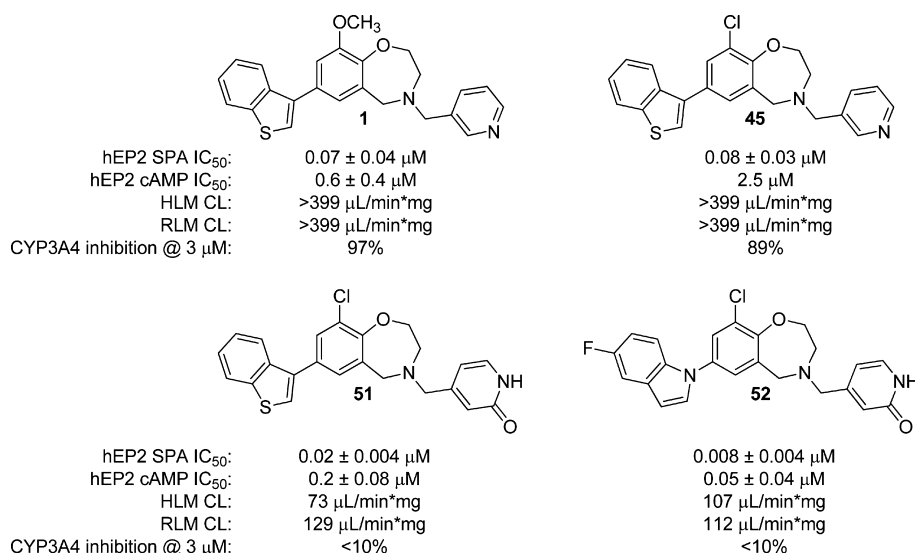
Figure 1. Human EP2 IC$_{50}$ values, microsomal stability, and CYP3A4 inhibition data for compounds **1**, **45**, **51**, and **52**. Data with SD are reported as the average of a minimum of two determinations.
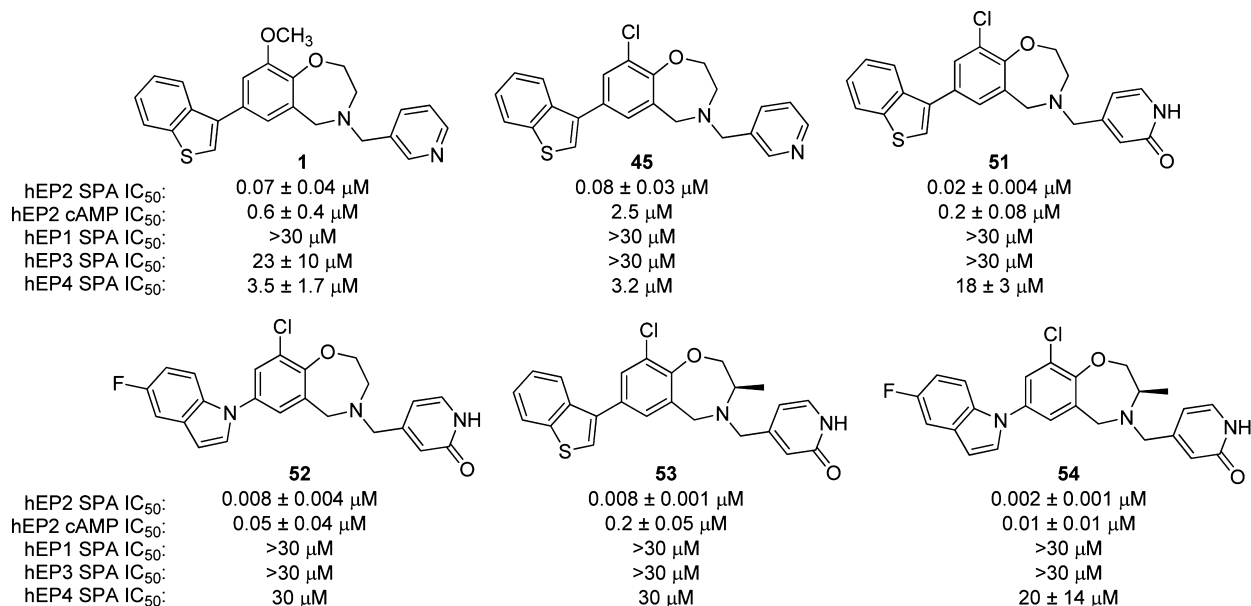
Figure 2. Human EP1, EP2, EP3, and EP4 IC$_{50}$ values for compounds **1**, **45**, and **51−54**. Data are reported as the average of a minimum of two determinations.

Table 6. Potency and Selectivity Data for 52

EP2 Potency[a]	
hEP2 SPA IC$_{50}$: 0.008 ± 0.004 μM	hEP2 cAMP IC$_{50}$: 0.05 ± 0.04 μM
rEP2 SPA IC$_{50}$: 0.01 ± 0.006 μM	rEP2 cAMP IC$_{50}$: 0.03 ± 0.01 μM
mEP2 SPA IC$_{50}$: 0.01 ± 0.003 μM	mEP2 cAMP IC$_{50}$: 0.004 ± 0.001 μM
Selectivity	
hDP Aeq IC$_{50}$: >33 μM	hTP Aeq IC$_{50}$: >33 μM
hIP Aeq IC$_{50}$: >33 μM	hCRTH2 Aeq IC$_{50}$: >33 μM

[a]Data are reported as the average of a minimum of two determinations.

Table 7. Pharmacokinetic Data for 52

CD-1 mouse PK (1.0 mg/kg iv)	CD-1 mouse PK (5.0 mg/kg po)
CL = 0.92 L/h/kg	AUC = 5.7 μM·h
$t_{1/2}$ = 3.4 h	C_{max} = 1.2 μM
V_{dss} = 2.6 L/kg	F = 44%
C57BL/6s mouse PK (200 mg/kg po)	**SD rat PK (100 mg/kg po)**
brain conc @ 2h = 11500 μg/L	brain conc @ 3h = 3440 μg/L
plasma conc @ 2h = 16400 μg/L	plasma conc @ 3h = 3920 μg/L

compound **52**. The results are shown in Figure 3, with mouse IC21 cells labeled red and Aβ peptide labeled green. Incubation with benzoxazepine **52** in a concentration range from 10 nM to 3.0 μM demonstrated a consistent dose-dependent increase in

the IC21-mediated phagocytosis of Aβ plaques present on brain slices (Figure 3D). The image of a brain slice incubated with 1 μM **52** (Figure 3C) clearly demonstrates an increase in Aβ phagocytosis compared to vehicle (Figure 3A), as shown by the reduction in the number and size of plaques and the internalization of Aβ by IC21 cells (green-labeled Aβ inside
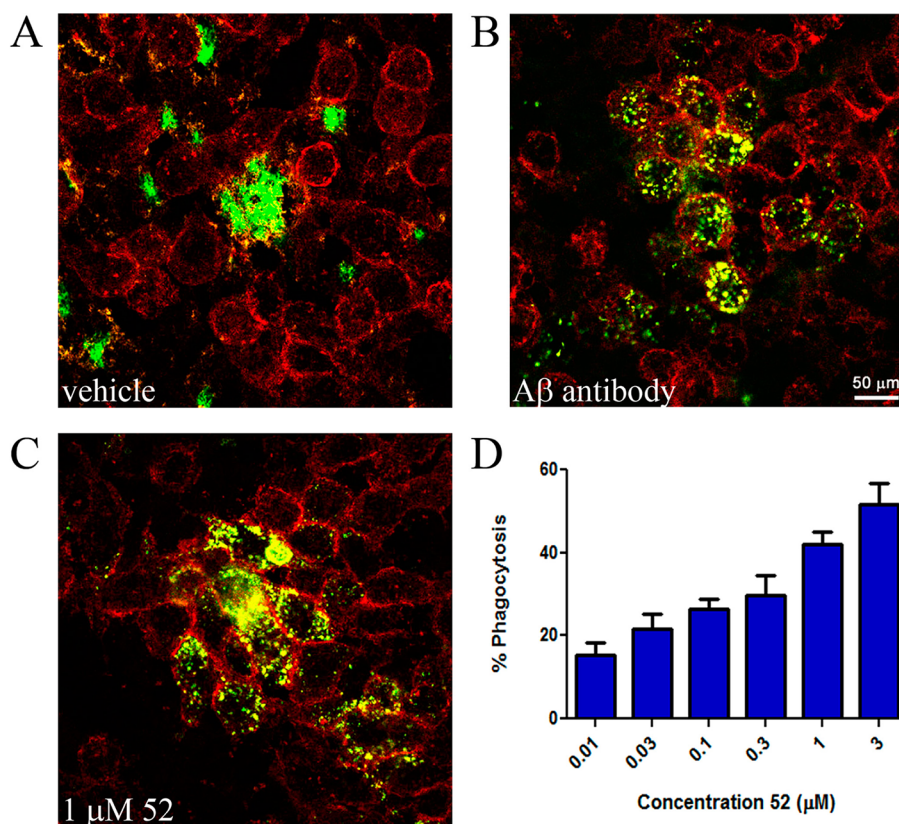
Figure 3. Images from the in vitro phagocytosis assay showing the incubation of brain slices from 18 month old Tg2576 mice incubated with mouse IC21 cells in the presence of (A) vehicle (DMSO), (B) 10 μg/mL Aβ antibody 2.1, (C) 1 μM compound **52**. (D) Dose−response of **52**.

Scheme 1[a]
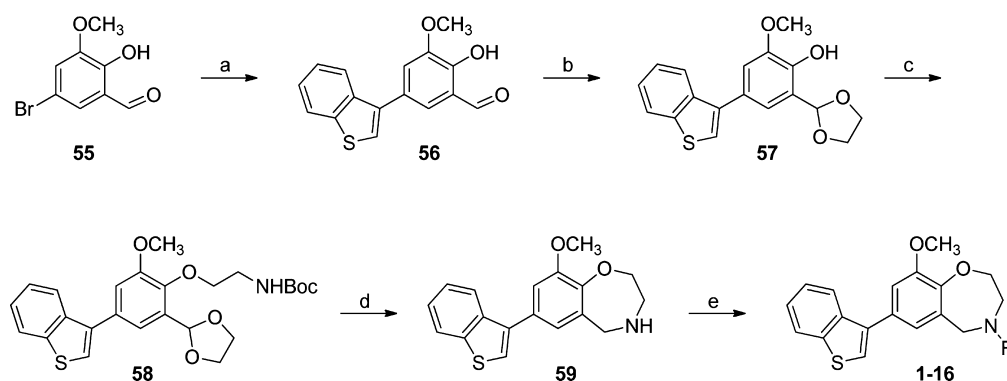
[a]Reagents and conditions: (a) benzo[b]thiophen-3-ylboronic acid, K₃PO₄, XPhos, Pd(OAc)₂, n-BuOH, 100 °C, 83%; (b) ethylene glycol, p-TsOH, toluene reflux, quant; (c) DEAD, PPh₃, THF rt, 65%; (d) (i) TFA, DCM, 91%, (ii) NaBH₄, MeOH, quant; (e) RCHO, NaBH(OAc)₃, dichloroethane, 15−98%.

red-labeled IC21 cells). The phagocytosis induced by compound **52** was similar to that caused by incubation with an Aβ antibody (Figure 3B).

■ **CHEMISTRY**

The preparation of analogues **1−16** began by introducing the benzothiophene ring through a Suzuki coupling employing Pd(OAc)₂ and XPhos to provide **56** in 83% yield (Scheme 1).[46] Protection of the aldehyde using ethylene glycol provided cyclic acetal **57** in quantitative yield followed by Mitsunobu reaction to provide the Boc-protected amine **58** in 65% yield. Formation of the oxazepine ring was accomplished by treating **58** with trifluoroacetic acid in dichloromethane followed by reduction

of the resulting cyclic imine using NaBH₄ in MeOH to provide benzoxazepine **59** in 91% yield over two steps. Finally, reductive amination using the corresponding aldehydes and NaBH-(OAc)₃ provided analogues **1−16**.

Nucleophilic displacement of mesylate **61**, prepared from alcohol **60** by phenol **55** provided the Boc-protected amine **62** in 81% yield (Scheme 2). Deprotection of the amine with TFA followed by reduction with NaBH₄ provided benzoxazepine **63** in 91% yield over two steps. Reductive amination of amine **63** with nicotinaldehyde provided the penultimate intermediate **64** in moderate yield. Palladium-catalyzed or copper-catalyzed coupling using bromide **64** directly or following conversion to the corresponding boronic acid provided analogues **17−39**.

Scheme 2[a]
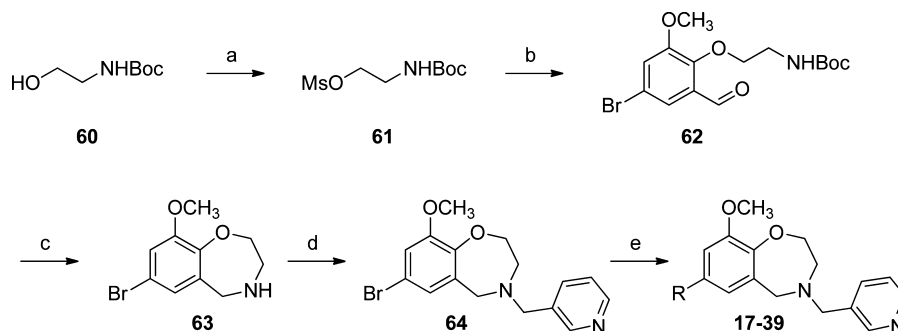
[a]Reagents and conditions: (a) MsCl, NEt$_3$, DCM, 0 °C−rt, quant; (b) **55**, K$_3$PO$_4$, DMF, 75 °C, 81%; (c) (i)TFA, DCM, rt, quant, (ii) NaBH$_4$, MeOH, 0 °C−rt, 91%; (d) nicotinaldehyde, NaBH(OAc)$_3$, DCM, rt, 45%; (e) RB(OH)$_2$, base, phosphine ligand, Pd catalyst, or (i) BuLi, triisopropylborate, THF, −78 °C, (ii) HCl, (iii) RX, K$_3$PO$_4$, XPhos, Pd(OAc)$_2$, *n*-butanol, 100 °C, or R$_2$NH, K$_3$PO$_4$, CuI, (1*S*,2*S*)-(+)-*N*,*N*′-dimethyl-1,2-cyclohexanediamine, dioxane, 110 °C.

Scheme 3[a]
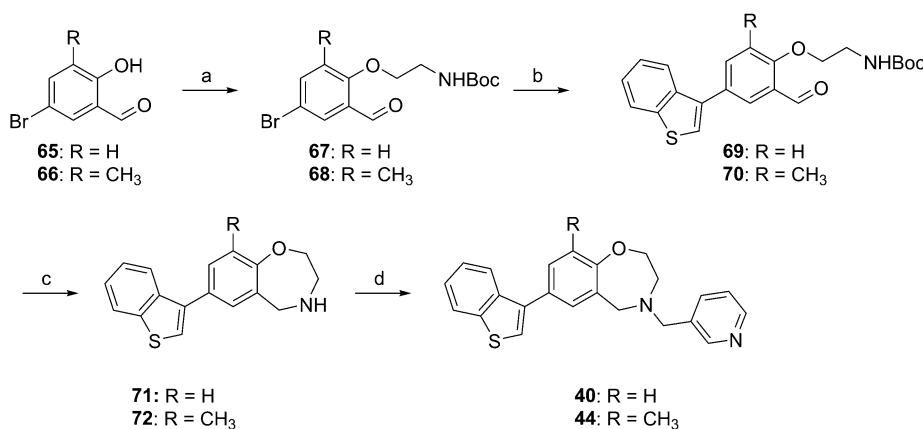
[a]Reagents and conditions: (a) **61**, K$_2$CO$_3$, DMF, rt−65 °C, 56−73%; (b) benzo[*b*]thiophen-3-ylboronic acid, Na$_2$CO$_3$, Pd(dppf)Cl$_2$·CH$_2$Cl$_2$, water, DMF, 80 °C, 81−87%; (c) (i)TFA, DCM, rt, quant, (ii) NaBH$_4$, EtOH, rt, quant; (d) nicotinaldehyde, NaBH(OAc)$_3$, DCM, rt, 50−67%.

Scheme 4[a]
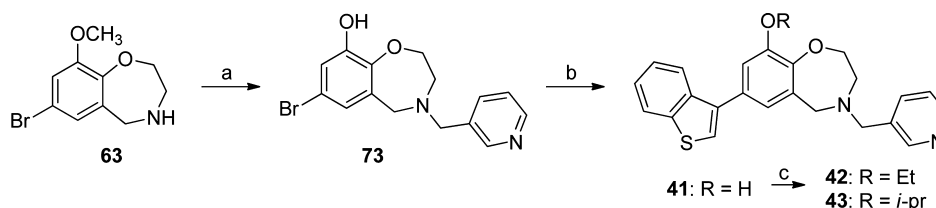
[a]Reagents and conditions: (a) (i) AlCl$_3$, octane-1-thiol, DCM rt, (ii) nicotinaldehyde, NaBH$_3$CN, 3 Å molecular sieves, MeOH, rt, 46%; (b) benzo[*b*]thiophen-3-ylboronic acid, Pd(OAc)$_2$, XPhos, K$_3$PO$_4$, *n*-butanol, 100 °C, 69%; (c) bromoethane or 2-bromopropane, NaH, DMF, rt, 9−44%.

The synthesis of analogues that replace the methoxy group of **1** with hydrogen **40** or methyl **44** was accomplished using similar chemistry as that used to prepare analogues **1−39** and is shown in Scheme 3. Nucleophilic addition of phenols **65** and **66** to mesylate **61** provided the Boc-protected amines **67** and **68** in good yield. Suzuki coupling with benzo[*b*]thiophen-3-ylboronic acid provided compounds **69** and **70** in 87% and 81% yield, respectively. Deprotection of the amines with TFA followed by reduction of the resulting imines using NaBH$_4$ in ethanol provided benzoxazepine **71** and **72** in quantitative yield. Reductive amination with nicotinaldehyde under standard conditions provided **40** and **44** in 50% and 67% yield, respectively.

Phenol **73** was prepared by demethylation of intermediate **63** using AlCl$_3$ and octanethiol followed by reductive amination with nicotinaldehyde (Scheme 4).[47] Suzuki coupling of **73** with benzo[*b*]thiophen-3-ylboronic acid provided phenol **41** in 69% yield. Alkylation of phenol **41** with ethyl bromide or isopropyl bromide using NaH in DMF provided ethyl ether **42** and isopropyl ether **43**.

Synthesis of chloride analogue **45** began by formylation of 4-bromo-2-chlorophenol **74** using the Duff reaction to provide **75** in 96% yield (Scheme 5). Protection of the aldehyde as the cyclic acetal followed by Mitsunobu reaction provided **77** in 65% yield. Suzuki coupling followed by deprotection of the amine and NaBH$_4$ reduction of the cyclic imine provided

Scheme 5[a]
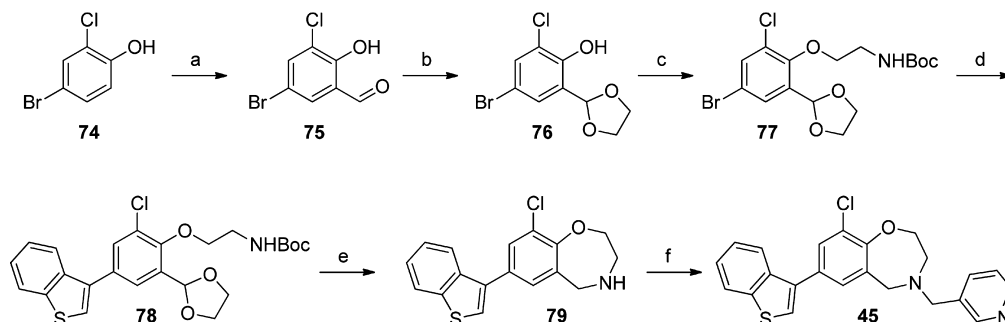
[a]Reagents and conditions: (a) hexamethylenetetramine, TFA, 90 °C, 96%; (b) ethylene glycol, *p*-TsOH, benzene reflux, 65%; (c) **60**, DEAD, PPh$_3$, THF, rt, 75%; (d) benzo[*b*]thiophen-3-ylboronic acid, Pd(OAc)$_2$, SPhos, K$_3$PO$_4$, *n*-butanol, 70 °C, 84%; (e) (i) TFA, DCM, rt, 62%, (ii) NaBH$_4$, MeOH, rt, 68%; (f) nicotinaldehyde, NaBH(OAc)$_3$, DCM, rt, 45%.

Scheme 6[a]
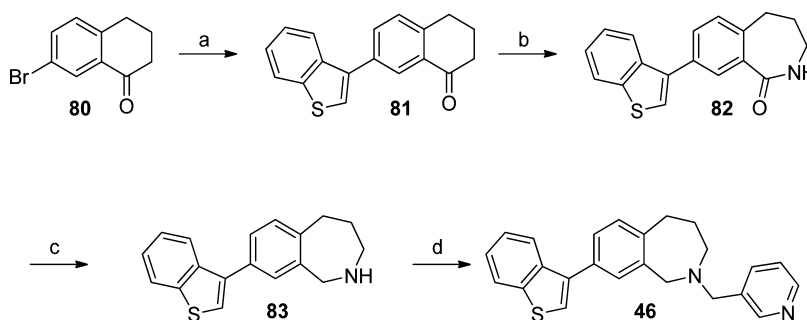
[a]Reagents and conditions: (a) benzo[*b*]thiophen-3-ylboronic acid, Pd(OAc)$_2$, XPhos, K$_3$PO$_4$, *n*-butanol, 100 °C, 88%; (b) NaN$_3$, TFA, HCl, THF, rt, 12%; (c) LAH, THF, 0 °C−rt, 50%; (d) nicotinaldehyde, NaBH(OAc)$_3$, DCM, rt, 44%.

Scheme 7[a]
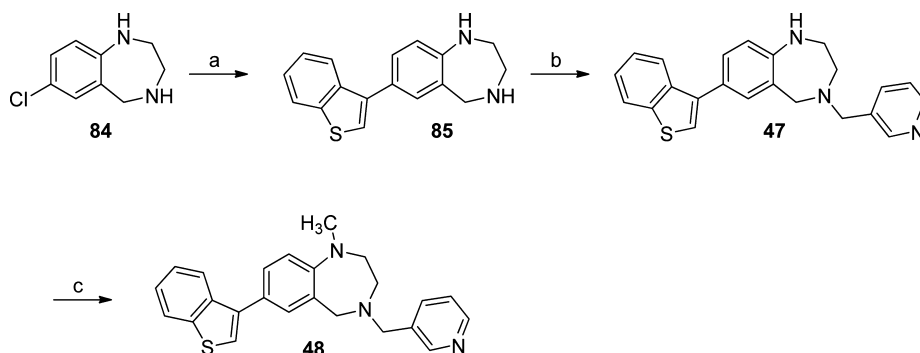
[a]Reagents and conditions: (a) benzo[*b*]thiophen-3-ylboronic acid, Pd(OAc)$_2$, XPhos, K$_3$PO$_4$, *n*-butanol, 100 °C, 51%; (b) nicotinaldehyde, NaBH(OAc)$_3$, DCM, rt, 53%; (c) formaldehyde, NaBH$_3$CN, 3 Å molecular sieves, MeOH, 33%.

benzoxazepine **79**. Reductive amination with nicotinaldehyde provided chloride analogue **45** in moderate yield.

Suzuki coupling of bromide **80** with benzo[*b*]thiophen-3-ylboronic acid provided **81** in 88% yield (Scheme 6). Ring expansion using sodium azide[48] followed by reduction of the resulting lactam with LAH provided benzoazepine **83**. Reductive amination with nicotinaldehyde gave benzoazepine core analogue **46** in moderate yield.

Preparation of benzodiazepine analogues **47** and **48** began with the Suzuki coupling of commercially available chloride **84** (Scheme 7). Reductive amination using nicotinaldehyde provided core analogue **47** in 53% yield. Methylated analogue **48** was obtained through the methylation of the

aniline nitrogen of **47** by reductive amination with form-aldehyde.

Alkylation of phenol **55** with ethyl bromoacetate provided ester **86** in excellent yield (Scheme 8). Introduction of the benzothiophene ring was accomplished using the standard Suzuki coupling procedure to provide **87** in 84% yield. The final step was achieved in a stepwise fashion by first forming the benzylamine intermediate through a reductive amination with pyridine-3-ylmethanamine at rt, followed by heating at reflux to effect ring closure and provide benzoxazapinone **49** in 73% yield.

The preparation of benzoxazapinone **50** began by oxidizing the aldehyde of intermediate **62** with sodium chlorite followed by methylation of the resulting acid with TMS−diazomethane

Scheme 8[a]
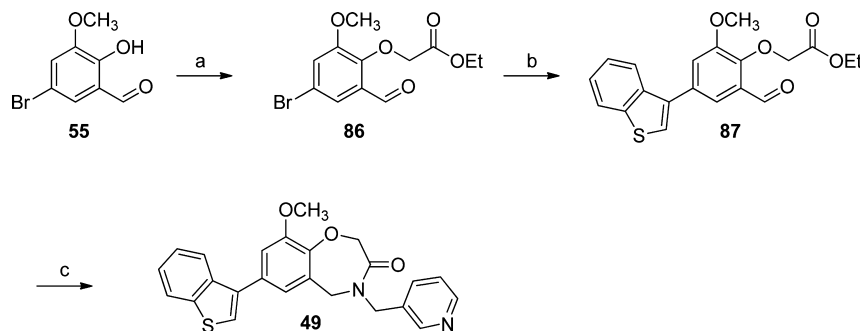
[a]Reagents and conditions: (a) ethyl bromoacetate, K$_2$CO$_3$, DMF rt, 91%; (b) benzo[*b*]thiophen-3-ylboronic acid, Pd(dppf)Cl$_2$·CH$_2$Cl$_2$, Na$_2$CO$_3$, water, DMF, 70 °C, 84%; (c) (i) pyridine-3-ylmethanamine, NaBH(OAc)$_3$, dichloroethane, rt, (ii) reflux, 73%.

Scheme 9[a]
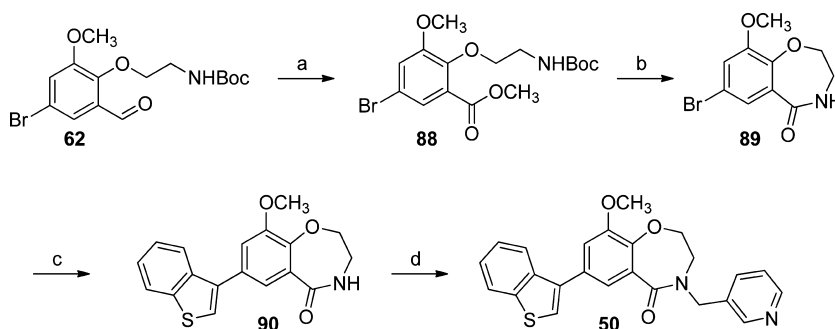
[a]Reagents and conditions: (a) (i) NaClO$_2$, sulfamic acid, dioxane, water, rt, 43%, (ii) TMSCHN$_2$, MeOH, DCM, 0 °C−rt, 46%; (b) (i) TFA, DCM, rt, (ii) DIPEA, MeOH, 65 °C, 52%; (c) benzo[*b*]thiophen-3-ylboronic acid, Pd(OAc)$_2$, XPhos, K$_3$PO$_4$, *n*-butanol, 100 °C, 57%; (d) 3-(bromomethyl)pyridine hydrobromide, NaH, THF, rt, 28%.

to yield methyl ester **88** (Scheme 9). Formation of the ring was accomplished by deprotection of the amine with TFA followed by cyclization under basic conditions. The benzothiophene ring was introduced via Suzuki coupling to provide the penultimate intermediate **90** in 57% yield. Alkylation of the lactam nitrogen was accomplished using NaH as the base providing core analogue **50**.

The synthesis of analogues **51**−**54** is shown in Scheme 10. Mitsunobu reactions employing the appropriate alcohols provided amines **77** with R = H and **91** with R = methyl. Treatment of the amines with trifluoroacetic acid in dichloromethane afforded imines **92** and **93** in quantitative yield. Benzothiophene analogue **94** was prepared by introducing the benzothiophene ring with a Suzuki coupling first, followed by reduction of the cyclic imine with NaBH$_4$ in MeOH. In contrast, indole analogues **95** and **96** were prepared by reducing the imine with NaBH$_4$ first, followed by introduction of the 5-fluoroindole ring through a copper-catalyzed coupling. Finally, reductive amination of amines **79** (from Scheme 7) and **94**−**96** with 2-hydroxyisonicotinaldehyde provided analogues **51**−**54** in good to moderate yield.

■ CONCLUSION

Herein we described the discovery of EP2 antagonist **1** from a HTS of our internal library. Lead compound **1** possessed a 70 nM binding affinity for the hEP2 receptor and a 600 nM IC$_{50}$ value in the hEP2 cAMP assay. It was a potent inhibitor of CYP3A4, had low microsomal stability, and lacked the exquisite selectivity against the hEP3 and hEP4 receptors that we desired. Subsequent modular SAR studies resulted in the discovery of

replacements for the benzothiophene ring, pyridine ring, and methyl ether of **1** that addressed these liabilities. Combination of these replacements provided benzoxazepine **52** possessing 8 nM binding affinity for the hEP2 receptor and a 50 nM IC$_{50}$ value in the hEP2 cAMP assay. The improvement in hEP2 potency was accomplished while maintaining a similar molecular weight compared to **1** and lowering the cLogD$_{7.4}$ by more than 2 orders of magnitude (cLogD$_{7.4}$ of 5.26 vs 2.79). Compound **52** was devoid of CYP inhibition at 3 *μ*M, had ~4000-fold higher binding affinity for the hEP2 receptor compared to the hEP1, hEP3, and hEP4 receptors, and was greater than 660-fold more potent in the hEP2 cAMP assay compared to functional assays for the human DP, TP, IP, and CRTH2 receptors. Benzoxazepine **52** was shown to have moderate clearance and good exposure in CD-1 mice and good CNS exposure in both C57Bl/6s mice and Sprague−Dawley rats. Finally, **52** demonstrated the ability to increase the macrophage-mediated phagocytosis of A*β* plaques present on mouse brain slices. To our knowledge, this is the first example of an EP2 antagonist eliciting an increase in A*β* phagocytosis in a similar manner to that caused by EP2 knockout microglia.

■ EXPERIMENTAL SECTION

All solvents and chemicals used were reagent grade. Anhydrous solvents were purchased from Aldrich and used as such. Analytical thin layer chromatography (TLC) and flash chromatography were performed on Merck silica gel 60 (230−400 mesh). Removal of solvents was conducted by using a rotary evaporator, and residual solvent was removed from nonvolatile compounds using a vacuum manifold maintained at approximately 1 Torr. All yields reported are

Scheme 10[a]
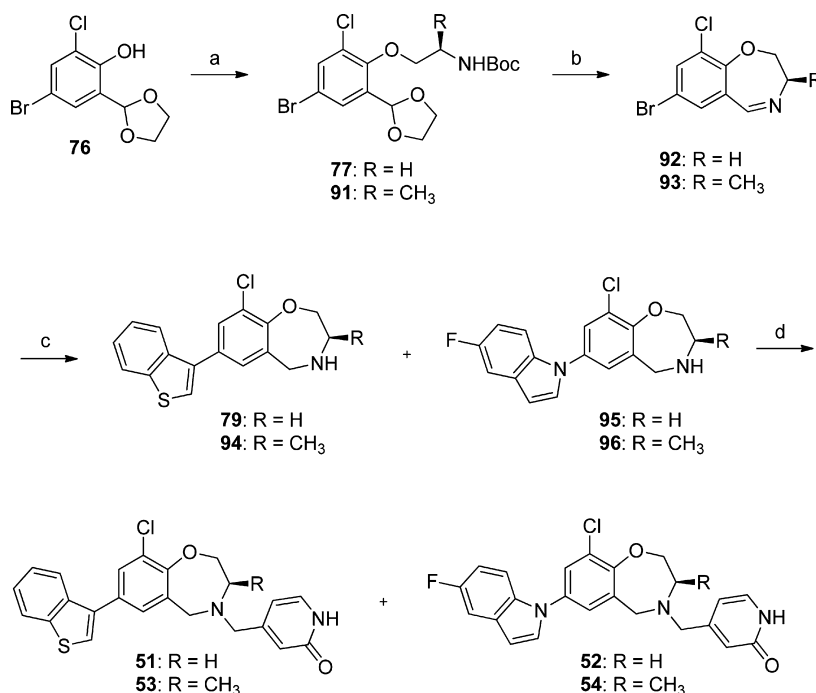
[a]Reagents and conditions: (a) **60** or (*R*)-*tert*-butyl 1-hydroxypropan-2-ylcarbamate, DEAD, PPh₃, THF rt, 75−79%; (b) TFA, DCM, rt, quant; (c) (i) benzo[*b*]thiophen-3-ylboronic acid, Pd(OAc)₂, SPhos, K₃PO₄, *n*-butanol, 100 °C, 76%, (ii) NaBH₄, MeOH, rt, quant (**94**), or (i) NaBH₄, MeOH, rt, 72−92%, (ii) 5-fluoro-1*H*-indole, (1*S*,2*S*)-(+)-*N*,*N*′-dimethyl-1,2-cyclohexanediamine, CuI, K₃PO₄, dioxane, 110 °C, 78%−quant (**95** and **96**); (d) 2-hydroxyisonicotinaldehyde, NaBH(OAc)₃, dichloroethane, rt, 33−92%.

isolated yields. Preparative reversed-phase−high pressure liquid chromatography (RP−HPLC) was performed using an Agilent 1100 series HPLC and Phenomenex Gemini C18 column (5 μm, 100 mm × 30 mm i.d.), eluting with a binary solvent system A and B using a gradient elution [A, H₂O with 0.1% TFA; B, CH₃CN with 0.1% TFA] with UV detection at 220 nm. All final compounds were purified to ≥95% purity as determined by an Agilent 1100 series HPLC with UV detection at 220 nm using the following method: Zorbax SB-C8 column (3.5 μm, 150 mm × 4.6 mm i.d.), eluting with a binary solvent system A and B using a 5−95% B (0−15 min) gradient elution [A, H₂O with 0.1% TFA; B, CH₃CN with 0.1% TFA]; flow rate 1.5 mL/min. Mass spectral data was recorded on an Agilent 1100 series LCMS with UV detection at 254 nm. NMR spectra were recorded on a Varian Gemini 400 MHz or Bruker Avance 500 MHz NMR spectrometer. Chemical shifts (δ) are reported in parts per million (ppm) relative to residual undeuterated solvent as internal reference and coupling constants (*J*) are reported in hertz (Hz). Splitting patterns are indicated as follows: s = singlet; d = doublet; t = triplet; q = quartet; qn = quintet; dd = doublet of doublet; dt = doublet of triplets; td = triplet of doublets; m = multiplet; br = broad peak.

General Procedure for the Preparation of Benzoxazepines 1−16. Sodium triacetoxyborohydride (1.25 equiv) was added to a 0.1 M solution of benzoxazepine **59** (1 equiv) and the corresponding aldehyde (1 equiv) in dichloroethane at rt. The reaction mixture was concentrated in vacuo once the reaction was deemed complete by TLC or LCMS. Purification by flash column chromatography provided the desired products.

7-(Benzo[*b*]thiophen-3-yl)-9-methoxy-4-(pyridin-3-ylmeth-yl)-2,3,4,5-tetrahydrobenzo[*f*][1,4]oxazepine (1). Following the general reductive amination procedure using nicotinaldehyde provided the title compound as a white solid in 61% yield. ¹H NMR (CDCl₃) δ 3.25 (m, 2H), 3.83 (m, 2H), 3.95 (s, 3H), 3.99 (m, 2H), 4.28 (m, 2H), 6.83 (d, *J* = 2.0 Hz, 1H), 7.12 (m, 1H), 7.34 (m, 1H), 7.40 (s, 1H), 7.44−7.41 (m, 2H), 7.95−7.89 (m, 3H), 8.58 (m, 2H). ESIMS *m/z* (rel intensity) 403.0 ([M + H], 100).

7-(Benzo[*b*]thiophen-3-yl)-9-methoxy-4-(pyridin-2-ylmeth-yl)-2,3,4,5-tetrahydrobenzo[*f*][1,4]oxazepine (2). Following the general reductive amination procedure using 2-pyridinecarboxaldehyde provided the title compound as an off-white solid in 53% yield. ¹H NMR (CDCl₃) δ 3.22 (m, 2H), 3.89 (s, 2H), 3.93 (s, 3H), 3.97 (s, 2H), 4.25 (m, 2H), 6.85 (d, *J* = 2.0 Hz, 1H), 7.06 (d, *J* = 2.0 Hz, 1H), 7.19 (m, 1H), 7.36 (s, 1H), 7.42−7.39 (m, 2H), 7.47 (d, *J* = 7.8 Hz, 1H), 7.68 (dt, *J* = 1.8 and 7.7 Hz, 1H), 7.93−7.91 (m, 2H), 8.60 (m, 1H). ESIMS *m/z* (rel intensity) 403.0 ([M + H], 100).

7-(Benzo[*b*]thiophen-3-yl)-9-methoxy-4-(pyridin-4-ylmeth-yl)-2,3,4,5-tetrahydrobenzo[*f*][1,4]oxazepine (3). Following the general reductive amination procedure using 4-pyridinecarboxaldehyde provided the title compound as an off-white solid in 39% yield. ¹H NMR (CDCl₃) δ 3.19 (m, 2H), 3.75 (s, 2H), 3.90 (s, 2H), 3.94 (s, 3H), 4.23 (m, 2H), 6.81 (d, *J* = 1.6 Hz, 1H), 7.08 (d, *J* = 1.6 Hz, 1H), 7.33 (d, *J* = 5.4 Hz, 2H), 7.36 (s, 1H), 7.41 (m, 2H), 7.93−7.88 (m, 2H), 8.57 (d, *J* = 5.6 Hz, 2H). ESIMS *m/z* (rel intensity) 403.0 ([M + H], 100).

7-(Benzo[*b*]thiophen-3-yl)-9-methoxy-4-(pyrimidin-5-yl-methyl)-2,3,4,5-tetrahydrobenzo[*f*][1,4]oxazepine (4). Following the general reductive amination procedure using pyrimidine-5-carboxaldehyde provided the title compound as a white solid in 24% yield. ¹H NMR (CDCl₃) δ 3.22 (m, 2H), 3.77 (m, 2H), 3.95 (s, 5H), 4.25 (m, 2H), 6.83 (d, *J* = 2.0 Hz, 1H), 7.11 (d, *J* = 2.0 Hz, 1H), 7.39 (s, 1H), 7.43 (m, 2H), 7.95−7.89 (m, 2H), 8.76 (s, 2H), 9.17 (s, 1H). ESIMS *m/z* (rel intensity) 404.0 ([M + H], 100).

7-(Benzo[*b*]thiophen-3-yl)-9-methoxy-4-((2-methoxypyri-din-3-yl)methyl)-2,3,4,5-tetrahydrobenzo[*f*][1,4]oxazepine (5). Following the general reductive amination procedure using 2-methoxynicotinaldehyde provided the title compound as a white solid in 61% yield. ¹H NMR (CDCl₃) δ 3.18 (m, 2H), 3.70 (s, 2H), 3.94 (br s, 8H), 4.25 (m, 2H), 6.89 (m, 2H), 7.08 (s, 1H), 7.37 (s, 1H), 7.40 (m, 2H), 7.73 (d, *J* = 6.7 Hz, 1H), 7.91 (m, 2H), 8.09 (m, 1H). ESIMS *m/z* (rel intensity) 433.1 ([M + H], 100).

7-(Benzo[*b*]thiophen-3-yl)-9-methoxy-4-((6-methoxypyridin-3-yl)methyl)-2,3,4,5-tetrahydrobenzo[*f*][1,4]oxazepine (6). Following the general reductive amination procedure using 6-methoxynico-tinaldehyde provided the title compound as a white solid in 75% yield.

^{1}H NMR (CDCl$_3$) δ 3.16 (m, 2H), 3.67 (s, 2H), 3.91 (s, 2H), 3.94 (s, 3H), 3.96 (s, 3H), 4.23 (m, 2H), 6.76 (d, J = 8.6 Hz, 1H), 6.86 (s, 1H), 7.09 (s, 1H), 7.39 (s, 1H), 7.42 (m, 2H), 7.67 (m, 1H), 7.93 (m, 2H), 8.07 (s, 1H). ESIMS m/z (rel intensity) 433.1 ([M + H], 100).

5-((7-(Benzo[b]thiophen-3-yl)-9-methoxy-2,3-dihydrobenzo-[f][1,4]oxazepin-4(5H)-yl)methyl)pyridin-2-ol (7). Following the general reductive amination procedure using 6-hydroxynicotinaldehyde provided the title compound as a white solid in 15% yield. ^{1}H NMR (CDCl$_3$) δ 3.14 (m, 2H), 3.48 (s, 2H), 3.87 (s, 2H), 3.92 (s, 3H), 4.19 (m, 2H), 6.60 (d, J = 9.3 Hz, 1H), 6.84 (s, 1H), 7.08 (s, 1H), 7.27 (s, 1H), 7.39 (m, 3H), 7.57 (d, J = 9.3 Hz, 1H), 7.90 (t, J = 7.1 Hz, 2H), 12.94 (br s, 1H). ESIMS m/z (rel intensity) 312.1 ([(M − CH$_2$C$_5$H$_4$NO) + H], 100), 419.0 ([M + H], 20).

7-(Benzo[b]thiophen-3-yl)-4-benzyl-9-methoxy-2,3,4,5-tetrahydrobenzo[f][1,4]oxazepine (8). Following the general reductive amination procedure using benzaldehyde provided the title compound as a white solid in 64% yield. ^{1}H NMR (CD$_3$OD) δ 3.30 (m, 2H), 3.65 (m, 2H), 3.93 (s, 3H), 4.52 (br s, 2H), 4.59 (br s, 2H), 7.13 (d, J = 1.7 Hz, 1H), 7.34 (d, J = 2.0 Hz, 1H), 7.42 (m, 2H), 7.52 (m, 3H), 7.57 (m, 2H), 7.61 (s, 1H), 7.90 (m, 1H), 7.96 (m, 1H). ESIMS m/z (rel intensity) 402.1 ([M + H], 100).

7-(Benzo[b]thiophen-3-yl)-4-(4-chlorobenzyl)-9-methoxy-2,3,4,5-tetrahydrobenzo[f][1,4]oxazepine (9). Following the general reductive amination procedure using 4-chlorobenzaldehyde provided the title compound as a white solid in 49% yield. ^{1}H NMR (CDCl$_3$) δ 3.15 (m, 2H), 3.69 (s, 2H), 3.88 (s, 2H), 3.93 (s, 3H), 4.21 (m, 2H), 6.82 (d, J = 2.0 Hz, 1H), 7.07 (d, J = 2.0 Hz, 1H), 7.31 (br s, 4 H), 7.36 (s, 1H), 7.41 (m, 2H), 7.91 (m, 2H).

7-(Benzo[b]thiophen-3-yl)-9-methoxy-4-(4-methylbenzyl)-2,3,4,5-tetrahydrobenzo[f][1,4]oxazepine (10). Following the general reductive amination procedure using 4-methylbenzaldehyde provided the title compound as an off-white solid in 52% yield. ^{1}H NMR (DMSO-d$_6$) δ 2.33 (s, 3H), 3.48 (br s, 2H), 3.88 (s, 3H), 4.14 (m, 1H), 4.34 (m, 1H), 4.54 (m, 4H), 7.18 (s, 1H), 7.28 (d, J = 7.8 Hz, 2H), 7.32 (s, 1H), 7.46 (m, 2H), 7.51 (d, J = 7.5 Hz, 2H), 7.84 (s, 1H), 8.00 (m, 1H), 8.08 (m, 1H).

7-(Benzo[b]thiophen-3-yl)-9-methoxy-4-(4-methoxybenzyl)-2,3,4,5-tetrahydrobenzo[f][1,4]oxazepine (11). Following the general reductive amination procedure using p-anisaldehyde provided the title compound as a white solid in 95% yield. ^{1}H NMR (CDCl$_3$) δ 3.14 (m, 2H), 3.67 (s, 2H), 3.81 (s, 3H), 3.88 (s, 2H), 3.93 (s, 3H), 4.21 (m, 2H), 6.85 (m, 1H), 6.88 (d, J = 8.2 Hz, 2H), 7.06 (m, 1H), 7.28 (d, J = 8.2 Hz, 2H), 7.36 (s, 1H), 7.41 (m, 2H), 7.92 (m, 2H).

Methyl 4-((7-(Benzo[b]thiophen-3-yl)-9-methoxy-2,3-dihydrobenzo[f][1,4]oxazepin-4(5H)-yl)methyl)benzoate (12). Following the general reductive amination procedure using methyl 4-formylbenzoate provided the title compound as a white solid in 25% yield. ^{1}H NMR (CDCl$_3$) δ 3.18 (m, 2H), 3.78 (s, 2H), 3.89 (s, 2H), 3.92 (s, 3H), 3.93 (s, 3H), 4.23 (m, 2H), 6.80 (d, J = 1.7 Hz, 1H), 7.07 (d, J = 1.7 Hz, 1H), 7.36 (s, 1H), 7.41 (m, 2H), 7.46 (d, J = 8.1 Hz, 2H), 7.91 (m, 2H), 8.02 (d, J = 8.3 Hz, 2H). ESIMS m/z (rel intensity) 460.1 ([M + H], 100).

4-((7-(Benzo[b]thiophen-3-yl)-9-methoxy-2,3-dihydrobenzo-[f][1,4]oxazepin-4(5H)-yl)methyl)benzonitrile (13). Following the general reductive amination procedure using methyl 4-formylbenzonitrile provided the title compound as a white solid in 83% yield. ^{1}H NMR (CDCl$_3$) δ 3.17 (m, 2H), 3.78 (s, 2H), 3.88 (s, 2H), 3.93 (s, 3H), 4.22 (m, 2H), 6.79 (s, 1H), 7.08 (s, 1H), 7.36 (s, 1H), 7.41 (m, 2H), 7.50 (d, J = 7.8 Hz, 2H), 7.63 (d, J = 7.8 Hz, 2H), 7.90 (m, 2H). ESIMS m/z (rel intensity) 427.1 ([M + H], 100).

7-(Benzo[b]thiophen-3-yl)-9-methoxy-4-(4-(methylsulfonyl)-benzyl)-2,3,4,5-tetrahydrobenzo[f][1,4]oxazepine (14). Following the general reductive amination procedure using 4-(methylsulfonyl)-benzaldehyde provided the title compound as a white solid in 55% yield. ^{1}H NMR (CDCl$_3$) δ 3.06 (s, 3H), 3.21 (m, 2H), 3.85 (s, 2H), 3.94 (s, 5H), 4.24 (m, 2H), 6.82 (d, J = 2.0 Hz, 1H), 7.09 (d, J = 2.0 Hz, 1H), 7.37 (s, 1H), 7.42 (m, 2H), 7.60 (d, J = 8.1 Hz, 2H), 7.88 (m, 1H), 7.92 (m, 3H). ESIMS m/z (rel intensity) 480.1 ([M + H], 100).

7-(Benzo[b]thiophen-3-yl)-4-(3-chlorobenzyl)-9-methoxy-2,3,4,5-tetrahydrobenzo[f][1,4]oxazepine (15). Following the general reductive amination procedure using 3-chlorobenzaldehyde

provided the title compound as a white solid in 70% yield. ^{1}H NMR (MeOD) δ 3.33 (m, 2H), 3.64 (m, 2H), 3.94 (s, 3H), 4.49 (br s, 2H), 4.57 (s, 2H), 7.13 (s, 1H), 7.34 (s, 1H), 7.42 (m, 2H), 7.50 (m, 3H), 7.61 (s, 1H), 7.64 (s, 1H), 7.92 (m, 1H), 7.95 (m, 1H). ESIMS m/z (rel intensity) 436.1 ([M + H], 100).

3-((7-(Benzo[b]thiophen-3-yl)-9-methoxy-2,3-dihydrobenzo-[f][1,4]oxazepin-4(5H)-yl)methyl)benzonitrile (16). Following the general reductive amination procedure using 3-formylbenzonitrile provided the title compound as a white solid in 98% yield. ^{1}H NMR (CDCl$_3$) δ 3.17 (m, 2H), 3.76 (s, 2H), 3.89 (s, 2H), 3.94 (s, 3H), 4.23 (m, 2H), 6.79 (d, J = 1.5 Hz, 1H), 7.08 (d, J = 1.5 Hz, 1H), 7.37 (s, 1H), 7.50−7.39 (m, 3H), 7.58 (m, 2H), 7.72 (s, 1H), 7.90 (m, 2H). ESIMS m/z (rel intensity) 427.1 ([M + H], 100).

General Procedure A for the Preparation of Benzoxazepines 17 and 23−26.[36] A round-bottomed flask was charged with a boronic acid (1.0 equiv), aryl bromide **64** (1.0 equiv), K$_3$PO$_4$ (3.0 equiv), phosphine ligand, and palladium catalyst. The flask was purged with nitrogen, and n-butanol (1 mL/0.1 mol **64**) was added. The reaction mixture was heated at 100 °C for 12 h, cooled to rt, filtered through Celite, and washed with EtOAc. The filtrate was concentrated in vacuo and purified by flash chromatography on silica gel or by reverse phase HPLC.

General Procedure B for the Preparation of Benzoxazepines 18−22.[36] A round-bottomed flask was charged with a boronic acid (1 equiv), aryl bromide **64** (1 equiv), Na$_2$CO$_3$ (2.0 equiv), and SPhos (0.1 equiv). The reaction flask was purged with nitrogen followed by the addition of Pd$_2$dba$_3$ (0.1 equiv) and dioxane, water, and EtOH (8:2:1, 0.5 mL/0.1 mol **64**). The reaction flask was purged with nitrogen, and the reaction mixture was heated at 80 °C for 48 h. The reaction mixture was concentrated in vacuo and purified by flash chromatography on silica gel or reverse-phase HPLC.

General Procedure C for the Preparation of Benzoxazepines 27 and 30−31. Butyllithium (1.2 mL, 1.89 mmol) (1.5 M in hexanes) was added dropwise to a solution of **64** (440 mg, 1.26 mmol) in anhydrous THF (13 mL) at −78 °C, followed by the addition of triisopropyl borate (436 μL, 1.89 mmol). The reaction mixture was aged at −78 °C for 1 h, warmed to rt, and quenched with 1 M HCl (1.5 mL). The reaction mixture was concentrated in vacuo and purified by flash chromatography on silica gel to provide (9-methoxy-4-(pyridin-3-ylmethyl)-2,3,4,5-tetrahydrobenzo[f][1,4]oxazepin-7-yl)-boronic acid, which was used directly in the next step. A reaction vessel was charged with an arylhalide (1 equiv), (9-methoxy-4-(pyridin-3-ylmethyl)-2,3,4,5-tetrahydrobenzo[f][1,4]oxazepin-7-yl)boronic acid (1.0 equiv), K$_3$PO$_4$ (3.0 equiv), and XPhos (0.1 equiv). The reaction vessel was purged with nitrogen before adding n-butanol (1 mL/0.1 mol **65**) and Pd(OAc)$_2$ (0.05 equiv). The reaction vessel was purged with nitrogen and heated at 100 °C for 12 h. The reaction mixture was concentrated in vacuo and purified by flash chromatography on silica gel or by reverse-phase HPLC.

General Procedure D for the Preparation of Benzoxazepines 29 and 32−38.[49] An oven-dried reaction vessel was charged with **64** (1.0 equiv), an indole (1.5 equiv), K$_3$PO$_4$ (2.2 equiv), and CuI (0.1 equiv). The reaction vessel was purged with nitrogen before adding (1S,2S)-(+)-N,N′-dimethyl-1,2-cyclohexanediamine (0.2 equiv) and dioxane (1 mL/0.1 mol **64**) and then purged again. The reaction mixture was heated at 110 °C for 12 h, concentrated in vacuo, and purified by flash chromatography on silica gel.

9-Methoxy-4-(pyridin-3-ylmethyl)-7-(thiophen-3-yl)-2,3,4,5-tetrahydrobenzo[f][1,4]oxazepine (17). Following general procedure A using thiophene-3-boronic acid, XPhos (0.1 equiv), and Pd(OAc)$_2$ (0.05 equiv) provided the title compound as a white solid in 34% yield. ^{1}H NMR (CD$_3$CN) δ 3.59 (m, 2H), 3.91 (s, 3H), 4.28 (m, 2H), 4.45 (s, 2H), 4.53 (s, 2H), 7.13 (d, J = 2.4 Hz, 1H), 7.36 (d, J = 2.0 Hz, 1H), 7.44 (dd, J = 5.1 and 1.6 Hz, 1H), 7.50 (dd, J = 5.1 and 2.7 Hz, 1H), 7.61 (m, 1H), 7.98 (dd, J = 8.0 and 5.7 Hz, 1H), 8.53 (d, J = 7.8 Hz, 1H), 8.83 (d, J = 5.1 Hz, 1H), 8.91 (s, 1H). ESIMS m/z (rel intensity) 353.0 ([M + H], 100).

7-(Benzo[b]thiophen-2-yl)-9-methoxy-4-(pyridin-3-ylmethyl)-2,3,4,5-tetrahydrobenzo[f][1,4]oxazepine (18). Following general procedure B using benzo[b]thiophen-2-ylboronic acid provided the

title compound as a white solid in 97% yield. ^{1}H NMR (MeOD) δ 3.35 (m, 2H), 3.78 (m, 2H), 3.97 (s, 3H), 4.40 (m, 2H), 4.71 (s, 2H), 7.35 (m, 3H), 7.51 (s, 1H), 7.71 (s, 1H), 7.84 (m, 2H), 8.19 (s, 1H), 8.88 (s, 1H), 9.01 (s, 1H), 9.22 (s, 1H). ESIMS m/z (rel intensity) 403.1 ([M + H], 100).

9-Methoxy-7-phenyl-4-(pyridin-3-ylmethyl)-2,3,4,5-tetrahydrobenzo[*f*][1,4]oxazepine (19). Following general procedure B using phenylboronic acid provided the title compound as a white solid in 99% yield. ^{1}H NMR (CD$_3$CN) δ 3.62 (m, 2H), 3.92 (s, 3H), 4.31 (m, 2H), 4.51 (s, 2H), 4.59 (s, 2H), 7.11 (d, J = 2.0 Hz, 1H), 7.35 (d, J = 2.0 Hz, 1H), 7.39 (m, 1H), 7.47 (m, 2H), 7.63 (m, 2H), 8.04 (dd, J = 5.8 and 8.0 Hz, 1H), 8.61 (m, 1H), 8.85 (m, 1H), 8.95 (s, 1H).

9-Methoxy-7-(naphthalen-1-yl)-4-(pyridin-3-ylmethyl)-2,3,4,5-tetrahydrobenzo[*f*][1,4]oxazepine (20). Following general procedure B using naphthalen-1-ylboronic acid provided the TFA salt of the title compound as a white solid in 81% yield. ^{1}H NMR (D$_2$O) δ 3.67 (s, 3H), 3.74 (m, 2H), 4.33 (s, 2H), 4.34 (m, 2H), 4.63 (s, 2H), 6.69 (d, J = 1.6 Hz, 1H), 7.00 (d, J = 1.6 Hz, 1H), 7.25 (d, J = 6.3 Hz, 1H), 7.35 (m, 1 H), 7.46 (m, 2H), 7.66 (d, J = 8.6 Hz, 1H), 7.86 (d, J = 8.2 Hz, 1H), 7.90 (d, J = 8.2 Hz, 1H), 8.08 (dd, J = 5.9 and 8.2 Hz, 1H), 8.63 (dt, J = 1.6 and 8.6 Hz, 1H), 8.87 (d, J = 5.1 Hz, 1H), 8.92 (d, J = 1.6 Hz, 1H). ESIMS m/z (rel intensity) 397.1 ([M + H], 100).

9-Methoxy-4-(pyridin-3-ylmethyl)-7-(o-tolyl)-2,3,4,5-tetrahydrobenzo[*f*][1,4]oxazepine (21). Following general procedure B using o-tolylboronic acid provided the title compound as a white solid in 78% yield. ^{1}H NMR (CD$_3$CN) δ 2.26 (s, 3H), 3.08 (m, 2H), 3.67 (s, 2H), 3.80 (m, 2H), 3.82 (s, 3H), 4.06 (m, 2H), 6.53 (d, J = 2.0 Hz, 1H), 6.87 (d, J = 2.0 Hz, 1H), 7.30−7.19 (m, 5H), 7.69 (m, 1H), 8.45 (m, 2H). ESIMS m/z (rel intensity) 361.1 ([M + H], 100).

9-Methoxy-4-(pyridin-3-ylmethyl)-7-(m-tolyl)-2,3,4,5-tetrahydrobenzo[*f*][1,4]oxazepine (22). Following general procedure B using m-tolylboronic acid provided the TFA salt of the title compound as a white solid in 89% yield. ^{1}H NMR (D$_2$O) δ 2.35 (s, 3H), 3.78 (m, 2H), 3.87 (s, 3H), 4.36 (m, 2H), 4.54 (s, 2H), 4.77 (s, 2H), 7.03 (s, 1H), 7.24 (m, 1H), 7.26 (s, 1H), 7.37 (m, 2H), 8.23 (m, 1H), 8.80 (d, J = 7.6 Hz, 1H), 8.97 (d, J = 5.9 Hz, 1H), 9.03 (s, 1H). ESIMS m/z (rel intensity) 361.1 ([M + H], 100).

9-Methoxy-4-(pyridin-3-ylmethyl)-7-(p-tolyl)-2,3,4,5-tetrahydrobenzo[*f*][1,4]oxazepine (23). Following general procedure A using 4-methylphenylboronic acid, XPhos (0.1 equiv), and Pd(OAc)$_2$ (0.05 equiv) provided the title compound as a white solid in 37% yield. ^{1}H NMR (CD$_3$CN) δ 2.39 (s, 3H), 3.09 (m, 2H), 3.70 (s, 2H), 3.86 (s, 2H), 3.90 (s, 3H), 4.07 (m, 2H), 6.87 (d, J = 2.2 Hz, 1H), 7.16 (d, J = 2.2 Hz, 1H), 7.28 (m, 2H), 7.34 (m, 1H), 7.51 (d, J = 8.0 Hz, 2H), 7.73 (dt, J = 7.8 and 2.0 Hz, 1H), 8.50 (m, 2H). ESIMS m/z (rel intensity) 361.1 ([M + H], 100).

7-(2-Chlorophenyl)-9-methoxy-4-(pyridin-3-ylmethyl)-2,3,4,5-tetrahydrobenzo[*f*][1,4]oxazepine (24). Following general procedure A using 2-chlorophenylboronic acid and Pd(dppf)Cl$_2$ (0.1 equiv) provided the title compound as a white solid in 95% yield. ^{1}H NMR (CDCl$_3$) δ 3.67 (m, 2H), 3.89 (s, 3H), 4.35 (m, 2H), 4.55 (s, 2H), 4.66 (s, 2H), 6.95 (d, J = 2.0 Hz, 1H), 7.24 (d, J = 2.0 Hz, 1H), 7.42 (m, 3H), 7.55 (m, 1H), 8.11 (dd, J = 7.8 and 5.9 Hz, 1H), 8.68 (d, J = 8.2 Hz, 1H), 8.87 (d, J = 5.5 Hz, 1H), 8.98 (s, 1H). ESIMS m/z (rel intensity) 381.1 ([M + H], 100).

7-(3-Chlorophenyl)-9-methoxy-4-(pyridin-3-ylmethyl)-2,3,4,5-tetrahydrobenzo[*f*][1,4]oxazepine (25). Following general procedure A using 3-chlorophenylboronic acid and Pd(dppf)Cl$_2$ (0.1 equiv) provided the title compound as a white solid in 64% yield. ^{1}H NMR (CD$_3$CN) δ 3.63 (m, 2H), 3.95 (s, 3H), 4.33 (m, 2H), 4.51 (s, 2H), 4.60 (s, 2H), 7.13 (d, J = 2.4 Hz, 1H), 7.36 (d, J = 2.4 Hz, 1H), 7.42 (m, 1H), 7.47 (t, J = 7.8 Hz, 1H), 7.58 (dt, J = 7.4 and 1.2 Hz, 1H), 7.68 (t, J = 1.8 Hz, 1H), 8.05 (m, 1H), 8.61 (d, J = 8.2 Hz, 1H), 8.88 (br s, 1H), 8.97 (br s, 1H). ESIMS m/z (rel intensity) 381.1 ([M + H], 100).

7-(4-Chlorophenyl)-9-methoxy-4-(pyridin-3-ylmethyl)-2,3,4,5-tetrahydrobenzo[*f*][1,4]oxazepine (26). Following general procedure A using 4-chlorophenylboronic acid and Pd(dppf)Cl$_2$

(0.1 equiv) provided the title compound as a white solid in 68% yield. ^{1}H NMR (CD$_3$CN) δ 3.63 (m, 2H) 3.94 (s, 3H) 4.33 (m, 2H) 4.50 (s, 2H) 4.58 (s, 2H) 7.10 (d, J = 2.4 Hz, 1H) 7.34 (d, J = 2.4 Hz, 1H) 7.50 (d, J = 8.6 Hz, 2H) 7.62 (d, J = 8.6 Hz, 2H) 8.04 (br s, 1 H) 8.59 (d, J = 8.2 Hz, 1H) 8.89 (br s, 1H) 8.96 (br s, 1H). ESIMS m/z (rel intensity) 381.1 ([M + H], 100).

7-(Benzo[*d*]isothiazol-3-yl)-9-methoxy-4-(pyridin-3-ylmethyl)-2,3,4,5-tetrahydrobenzo[*f*][1,4]oxazepine (27). Following general procedure C using 3-chlorobenzo[*d*]isothiazole provided the title compound as a white solid in 24% yield. ^{1}H NMR (CD$_3$CN) δ 3.12 (m, 2H), 3.74 (s, 2H), 3.91 (s, 2H), 3.92 (s, 3H), 4.14 (m, 2H), 7.14 (d, J = 2.2 Hz, 1H), 7.33 (ddd, J = 7.6, 4.7, and 0.6 Hz, 1H), 7.44 (d, J = 2.2 Hz, 1H), 7.55 (ddd, J = 1.0, 7.0, and 8.2 Hz, 1H), 7.64 (ddd, J = 1.0, 7.0, and 8.2 Hz, 1H), 7.74 (dt, J = 7.8 and 1.9 Hz, 1H), 8.13 (dt, J = 8.2 and 0.9 Hz, 1H), 8.23 (dt, J = 8.2 and 1.0 Hz, 1H), 8.53 (d, J = 1.8 Hz, 1H). ESIMS m/z (rel intensity) 404.2 ([M + H], 100).

7-(1*H*-Benzo[*d*]imidazol-1-yl)-9-methoxy-4-(pyridin-3-yl-methyl)-2,3,4,5-tetrahydrobenzo[*f*][1,4]oxazepine (28). To a glass vial containing CuI (2.7 mg, 0.014 mmol), benzimidazole (19 mg, 0.165 mmol), **64** (50 mg, 0.143 mmol), 8-hydroxyquinoline (2.1 mg, 0.014 mmol), and Cs$_2$CO$_3$ (47 mg, 0.143 mmol) was added DMF (1 mL) and water (0.1 mL).[50] The vial was purged with nitrogen, capped, and heated at 130 °C for 24 h. The reaction mixture was diluted with 1 M LiCl (2 mL) and extracted with EtOAc (3 × 2 mL). The organics were pooled, dried over Na$_2$SO$_4$, filtered, and concentrated in vacuo. Purification by reverse phase HPLC followed by neutralization of the product and filtration through a plug of silica gel provided the title compound as a white solid in 35% yield. ^{1}H NMR (CD$_3$CN) δ 3.13 (m, 2H), 3.74 (s, 2H), 3.89 (s, 2H), 3.90 (s, 3H), 4.12 (m, 2H), 6.87 (d, J = 2.5 Hz, 1H), 7.16 (d, J = 2.5 Hz, 1H), 7.35 (m, 3H), 7.60 (m, 1H), 7.76 (m, 2H), 8.19 (s, 1H), 8.48 (dd, J = 4.7 and 1.4 Hz, 1H), 8.52 (d, J = 1.4 Hz, 1H). ESIMS m/z (rel intensity) 387.2 ([M + H], 100).

7-(1*H*-Indol-1-yl)-9-methoxy-4-(pyridin-3-ylmethyl)-2,3,4,5-tetrahydrobenzo[*f*][1,4]oxazepine (29). Following general procedure D using indole provided the title compound as a white solid in 33% yield. ^{1}H NMR (CD$_3$CN) δ 3.12 (m, 2H), 3.73 (s, 2H), 3.88 (s, 2H), 3.89 (s, 3H), 4.11 (m, 2H), 6.69 (dd, J = 3.3 and 0.8 Hz, 1H), 6.80 (d, J = 2.4 Hz, 1H), 7.11 (d, J = 2.4 Hz, 1H), 7.16 (m, 1H), 7.24 (m, 1H), 7.33 (m, 1H), 7.45 (d, J = 3.3 Hz, 1H), 7.57 (m, 1H), 7.67 (dt, J = 8.0 and 0.9 Hz, 1H), 7.74 (dt, J = 7.7 and 2.0 Hz, 1H), 8.49 (dd, J = 4.7 and 1.6 Hz, 1H), 8.5 (d, J = 1.6 Hz, 1H). ESIMS m/z (rel intensity) 386.2 ([M + H], 100).

7-(1*H*-Indol-3-yl)-9-methoxy-4-(pyridin-3-ylmethyl)-2,3,4,5-tetrahydrobenzo[*f*][1,4]oxazepine (30). Following general procedure C using tert-butyl 3-bromo-1*H*-indole-1-carboxylate provided tert-butyl 3-(9-methoxy-4-(pyridin-3-ylmethyl)-2,3,4,5-tetrahydrobenzo-[*f*][1,4]oxazepin-7-yl)-1*H*-indole-1-carboxylate as a white solid in 45% yield. A solution of the Boc-protected indole and TFA (0.14 mL, 1.8 mmol) in DCM (1 mL) was stirred at rt for 12 h to provide the title compound as a white solid in 24% yield. ^{1}H NMR (CD$_3$CN) δ 3.00 (m, 2H), 3.62 (s, 2H), 3.77 (s, 2H), 3.81 (s, 3H), 3.97 (m, 2H), 6.83 (d, J = 2.0 Hz, 1H), 7.05 (m, 1H), 7.12 (m, 2H), 7.24 (ddd, J = 7.6, 4.7, and 0.6 Hz, 1H), 7.37 (d, J = 2.5 Hz, 1H), 7.40 (dt, J = 8.2 and 0.9 Hz, 1H), 7.64 (dt, J = 7.8 and 2.0 Hz, 1H), 7.77 (d, J = 8.4 Hz, 1H), 8.40 (dd, J = 4.7 and 1.8 Hz, 1H), 8.42 (d, J = 1.6 Hz, 1H), 9.36 (s, 1H). ESIMS m/z (rel intensity) 386.2 ([M + H], 100).

9-Methoxy-7-(1-methyl-1*H*-indol-3-yl)-4-(pyridin-3-ylmethyl)-2,3,4,5-tetrahydrobenzo[*f*][1,4]oxazepine (31). Following procedure C using 3-bromo-1*H*-indole provided the title compound as a white solid in 31% yield. ^{1}H NMR (CD$_3$CN) δ 3.35 (m, 2H), 3.86 (s, 3H), 3.93 (s, 3H), 4.10 (s, 2H), 4.19 (s, 2H), 4.20 (m, 2H), 7.04 (d, J = 2.0 Hz, 1H), 7.18 (m, 1H), 7.29 (m, 2H), 7.48−7.44 (m, 3H), 7.92 (m, 1H), 7.95 (dt, J = 8.0 and 1.9 Hz, 1H), 8.63 (m, 2H). ESIMS m/z (rel intensity) 400.3 ([M + H], 100).

7-(3-Chloro-1*H*-indol-1-yl)-9-methoxy-4-(pyridin-3-ylmethyl)-2,3,4,5-tetrahydrobenzo[*f*][1,4]oxazepine (32). Following general procedure D using 3-chloro-1*H*-indole provided the title compound as a white solid in 26% yield. ^{1}H NMR (CD$_3$CN) δ 3.12 (m, 2H), 3.73 (s, 2H), 3.87 (s, 2H), 3.88 (s, 3H), 4.11 (m, 2H), 6.79 (d, J = 2.5 Hz,

1H), 7.09 (d, J = 2.5 Hz, 1H), 7.27 (m, 1H), 7.33 (m, 2H), 7.53 (s, 1H), 7.58 (m, 1H), 7.66 (m, 1H), 7.74 (dt, J = 7.8 and 2.0 Hz, 1H), 8.49 (dd, J = 4.7 and 1.6 Hz, 1H), 8.52 (d, J = 1.8 Hz, 1H). ESIMS m/z (rel intensity) 420.1 ([M + H], 100).

7-(4-Chloro-1H-indol-1-yl)-9-methoxy-4-(pyridin-3-ylmethyl)-2,3,4,5-tetrahydrobenzo[f][1,4]oxazepine (33). Following general procedure D using 4-chloro-1H-indole provided the title compound as a white solid in 58% yield. ^{1}H NMR (CD$_3$CN) δ 3.13 (m, 2H), 3.75 (s, 2H), 3.88 (s, 3H), 3.89 (s, 2H), 4.12 (m, 2H), 6.76 (dd, J = 3.1 and 0.8 Hz, 1H), 6.79 (d, J = 2.8 Hz, 1H), 7.10 (d, J = 2.4 Hz, 1H), 7.19 (s, 1H), 7.20 (d, J = 2.0 Hz, 1H), 7.34 (dd, J = 7.6 and 4.9 Hz, 1H), 7.49 (m, 1H), 7.51 (d, J = 3.5 Hz, 1H), 7.76 (m, 1H), 8.50 (br s, 1H), 8.53 (br s, 1H). ESIMS m/z (rel intensity) 420.1 ([M + H], 100).

7-(5-Chloro-1H-indol-1-yl)-9-methoxy-4-(pyridin-3-ylmethyl)-2,3,4,5-tetrahydrobenzo[f][1,4]oxazepine (34). Following general procedure D using 5-chloro-1H-indole provided the title compound as a white solid in 65% yield. ^{1}H NMR (CD$_3$CN) δ 3.15 (m, 2H), 3.79 (s, 2H), 3.88 (s, 3H), 3.91 (s, 2H), 4.12 (m, 2H), 6.64 (dd, J = 3.1 and 0.8 Hz, 1H), 6.77 (d, J = 2.4 Hz, 1H), 7.08 (d, J = 2.8 Hz, 1H), 7.19 (dd, J = 8.8 and 2.2 Hz, 1H), 7.37 (m, 1H), 7.48 (d, J = 3.1 Hz, 1H), 7.51 (d, J = 8.6 Hz, 1H), 7.66 (d, J = 2.4 Hz, 1H), 7.78 (d, J = 7.8 Hz, 1H), 8.55 (m, 2H). ESIMS m/z (rel intensity) 420.1 ([M + H], 100).

7-(6-Chloro-1H-indol-1-yl)-9-methoxy-4-(pyridin-3-ylmethyl)-2,3,4,5-tetrahydrobenzo[f][1,4]oxazepine (35). Following general procedure D using 6-chloro-1H-indole provided the title compound as a white solid in 68% yield. ^{1}H NMR (CD$_3$CN) δ 3.17 (m, 2H), 3.81 (s, 2H), 3.88 (s, 3H), 3.93 (s, 2H), 4.14 (m, 2H), 6.68 (dd, J = 3.3 and 0.8 Hz, 1H), 6.80 (d, J = 2.4 Hz, 1H), 7.08 (d, J = 2.4 Hz, 1H), 7.14 (dd, J = 8.4 and 2.0 Hz, 1H), 7.40 (br s, 1H), 7.44 (d, J = 3.1 Hz, 1H), 7.55 (m, 1H), 7.63 (d, J = 8.4 Hz, 1H), 7.80 (d, J = 7.8 Hz, 1H), 8.5 (br s, 2H). ESIMS m/z (rel intensity) 420.1 ([M + H], 100).

7-(7-Chloro-1H-indol-1-yl)-9-methoxy-4-(pyridin-3-ylmethyl)-2,3,4,5-tetrahydrobenzo[f][1,4]oxazepine (36). Following general procedure D using 7-chloro-1H-indole provided the title compound as a white solid in 36% yield. ^{1}H NMR (CD$_3$CN) δ 3.13 (m, 2H), 3.70 (s, 2H), 3.83 (s, 3H), 3.85 (s, 2H), 4.11 (m, 2H), 6.69 (m, 2H), 7.04 (d, J = 2.4 Hz, 1H), 7.10 (dd, J = 7.8 and 7.6 Hz, 1H), 7.21 (dd, J = 7.6 and 1.2 Hz, 1H), 7.29 (m, 2H), 7.63 (dd, J = 7.9 and 1.1 Hz, 1H), 7.71 (dt, J = 7.8 and 1.9 Hz, 1H), 8.46 (br s, 1H), 8.50 (br s, 1H). ESIMS m/z (rel intensity) 420.1 ([M + H], 100).

1-(9-Methoxy-4-(pyridin-3-ylmethyl)-2,3,4,5-tetrahydrobenzo[f][1,4]oxazepin-7-yl)-1H-indole-5-carbonitrile (37). Following general procedure D using 1H-indole-5-carbonitrile provided the title compound as a white solid in 88% yield. ^{1}H NMR (CD$_3$CN) δ 3.43 (m, 2H), 3.90 (s, 3H), 4.24 (s, 2H), 4.26 (s, 2H), 4.27 (m, 2H), 6.82 (dd, J = 3.3 and 0.8 Hz, 1H), 6.95 (d, J = 2.4 Hz, 1H), 7.19 (d, J = 2.4 Hz, 1H), 7.51 (dd, J = 8.7 and 1.7 Hz, 1H), 7.61 (d, J = 3.3 Hz, 1H), 7.64 (br s, 1H), 7.68 (d, J = 8.6 Hz, 1H), 8.11 (d, J = 1.0 Hz, 1H), 8.15 (d, J = 7.8 Hz, 1H), 8.72 (br s, 2H). ESIMS m/z (rel intensity) 411.2 ([M + H], 100).

7-(5-Fluoro-1H-indol-1-yl)-9-methoxy-4-(pyridin-3-ylmethyl)-2,3,4,5-tetrahydrobenzo[f][1,4]oxazepine (38). Following general procedure D using 5-fluoro-1H-indole provided the title compound as a white solid in 82% yield. ^{1}H NMR (CD$_3$CN) δ 3.23 (m, 2H), 3.89 (s, 3H), 3.91 (s, 2H), 4.01 (s, 2H), 4.16 (m, 2H), 6.67 (d, J = 3.1 Hz, 1H), 6.83 (d, J = 2.5 Hz, 1H), 7.01 (td, J = 9.2 and 2.6 Hz, 1H), 7.12 (d, J = 2.5 Hz, 1H), 7.36 (dd, J = 9.8 and 2.5 Hz, 1H), 7.42 (dd, J = 7.7 and 5.0 Hz, 1H), 7.50 (d, J = 3.3 Hz, 1H), 7.54 (dd, J = 9.1 and 4.4 Hz, 1H), 7.87 (dt, J = 7.8 and 1.9 Hz, 1H), 8.56 (d, J = 3.9 Hz, 1H), 8.59 (s, 1H). ESIMS m/z (rel intensity) 404.2 ([M + H], 100).

7-(5-Chloroindolin-1-yl)-9-methoxy-4-(pyridin-3-ylmethyl)-2,3,4,5-tetrahydrobenzo[f][1,4]oxazepine (39). An oven-dried glass vial was charged with **64** (83 mg, 0.238 mmol), sodium tert-butoxide (69 mg, 0.713 mmol), 1,3-bis(2,6-diisopropylphenyl)-imidazolidine hydrochloride (10 mg, 0.024 mmol), and Pd(OAc)$_2$ (2.7 mg, 0.012 mmol). The vial was purged with nitrogen, dioxane (1.5 mL) and 5-chloroindoline (37 μL, 0.238 mmol) were added, the vial was purged with nitrogen again, and then capped and heated at 110 °C for 12 h. The reaction mixture was concentrated in vacuo and purified by flash chromatography on silica gel to provide the title compound as a white solid in 20% yield. ^{1}H NMR (CD$_3$CN) δ 3.08

(m, 2H), 3.09 (t, J = 8.5 Hz, 2H), 3.68 (s, 2H), 3.78 (s, 2H), 3.84 (s, 3H), 3.91 (t, J = 8.5 Hz, 2H), 4.01 (m, 2H), 6.46 (d, J = 2.7 Hz, 1H), 6.78 (d, J = 2.5 Hz, 1H), 6.94 (d, J = 8.4 Hz, 1H), 7.02 (dd, J = 8.4 and 2.2 Hz, 1H), 7.14 (m, 1H), 7.33 (dd, J = 7.7 and 4.8 Hz, 1H), 7.71 (dt, J = 7.8 and 1.9 Hz, 1H), 8.50 (m, 2H). ESIMS m/z (rel intensity) 422.2 ([M + H], 100).

7-(Benzo[b]thiophen-3-yl)-4-(pyridin-3-ylmethyl)-2,3,4,5-tetrahydrobenzo[f][1,4]oxazepine (40). NaBH(OAc)$_3$ (339 mg, 1.60 mmol) was added to a solution of **71** (300 mg, 1.07 mmol) and nicotinaldehyde (101 μL, 1.07 mmol) in dichloroethane (20 mL) at rt. The reaction mixture was aged at rt for 12 h before adding DCM (75 mL) and washing with saturated aqueous NaHCO$_3$ and brine. The solution was dried over MgSO$_4$, filtered, and concentrated in vacuo to provide an orange oil. Purification by flash chromatography on silica gel eluting with 2% MeOH/DCM provided a colorless oil that was dissolved in ether, and 1 M HCl in ether (1.4 mL) was added to provide the title compound as a white solid (218 mg, 50%). ^{1}H NMR (D$_2$O) δ 3.72 (m, 2H), 4.38 (m, 2H), 4.50 (s, 2H), 4.64 (s, 2H), 7.24 (d, J = 8.2 Hz, 1H), 7.38 (d, J = 2.0 Hz, 1H), 7.42 (m, 2H), 7.53 (s, 1H), 7.60 (dd, J = 8.2 and 2.0 Hz, 1H), 7.81 (m, 1H), 7.97 (m, 2H), 8.48 (d, J = 7.8 Hz, 1H), 8.80 (d, J = 4.7 Hz, 1H), 8.83 (s, 1H). ESIMS m/z (rel intensity) 373.0 ([M + H], 100).

7-(Benzo[b]thiophen-3-yl)-4-(pyridin-3-ylmethyl)-2,3,4,5-tetrahydrobenzo[f][1,4]oxazepin-9-ol (41). Following general procedure A using **73** and benzo[b]thiophen-3-ylboronic acid, XPhos (0.1 equiv), and Pd(OAc)$_2$ (0.05 equiv) provided the title compound as a white solid in 69% yield. ^{1}H NMR (CDCl$_3$) δ 3.19 (m, 2H), 3.75 (s, 2H), 3.90 (s, 2H), 4.18 (m, 2H), 6.74 (d, J = 2.2 Hz, 1H), 7.15 (d, J = 2.0 Hz, 1H), 7.31 (dd, J = 7.8 and 4.9 Hz, 1H), 7.34 (s, 1H), 7.38 (m, 2H), 7.76 (br d, J = 7.8 Hz, 1H), 7.90 (m, 2H), 8.55 (d, J = 4.2 Hz, 1H), 8.58 (s, 1H). ESIMS m/z (rel intensity) 389.0 ([M + H], 100).

7-(Benzo[b]thiophen-3-yl)-9-ethoxy-4-(pyridin-3-ylmethyl)-2,3,4,5-tetrahydrobenzo[f][1,4]oxazepine (42). NaH (60% in mineral oil) (4.2 mg, 0.106 mmol) was added to a solution of **41** (41 mg, 0.106 mmol) in anhydrous DMF (1 mL) at rt followed by the addition of bromoethane (8 μL, 0.106 mmol). The reaction mixture was stirred at rt for 12 h and diluted with water (2 mL), DCM (2 mL), and brine (1 mL). The layers were separated, and the aqueous layer was extracted with EtOAc. The organics were combined, dried over Na$_2$SO$_4$, filtered, and concentrated in vacuo. Purification by flash chromatography on silica gel eluting with 0−10% MeOH/DCM provided the title compound as a white solid (19.4 mg, 44%). ^{1}H NMR (CD$_3$CN) δ 1.39 (t, J = 6.9 Hz, 3H), 3.10 (m, 2H), 3.71 (s, 2H), 3.84 (s, 2H), 4.09 (m, 2H), 4.12 (q, J = 6.9 Hz, 2H), 6.83 (d, J = 2.2 Hz, 1H), 7.13 (d, J = 2.0 Hz, 1H), 7.31 (m, 1H), 7.43 (m, 2H), 7.51 (s, 1H), 7.72 (dt, J = 7.8 and 2.0 Hz, 1H), 7.93 (m, 1H), 7.96 (m, 1H), 8.46 (dd, J = 4.7 and 1.6 Hz, 1H), 8.50 (d, J = 1.7 Hz, 1H). ESIMS m/z (rel intensity) 417.3 ([M + H], 100).

7-(Benzo[b]thiophen-3-yl)-9-isopropoxy-4-(pyridin-3-yl-methyl)-2,3,4,5-tetrahydrobenzo[f][1,4]oxazepine (43). NaH (60% in mineral oil) (6.6 mg, 0.154 mmol) was added to a solution of **41** (60 mg, 0.154 mmol) in anhydrous DMF (1 mL) at rt followed by the addition of 2-bromopropane (15 μL, 0.154 mmol). The reaction mixture was stirred at rt for 12 h and diluted with water (2 mL), DCM (2 mL), and brine (1 mL). The layers were separated, and the aqueous layer was extracted with EtOAc. The organics were combined, dried over Na$_2$SO$_4$, filtered, and concentrated in vacuo. Purification by flash chromatography on silica gel eluting with 0−10% MeOH/DCM provided the title compound as a white solid (6.0 mg, 9%). ^{1}H NMR (CD$_3$CN) δ 1.33 (d, J = 6.1 Hz, 6H), 3.09 (m, 2H), 3.71 (s, 2H), 3.84 (s, 2H), 4.08 (m, 2H), 4.59 (sep, J = 6.1 Hz, 1H), 6.86 (d, J = 2.2 Hz, 1H), 7.14 (d, J = 2.2 Hz, 1H), 7.31 (m, 1H), 7.43 (m 2H), 7.51 (s, 1H), 7.72 (dt, J = 7.8 and 2.0 Hz, 1H), 7.90 (m, 1H), 7.97 (m, 1H), 8.47 (dd, J = 4.8 and 1.7 Hz, 1H), 8.50 (d, J = 1.6 Hz, 1H). ESIMS m/z (rel intensity) 431.2 ([M + H], 100).

7-(Benzo[b]thiophen-3-yl)-9-methyl-4-(pyridin-3-ylmethyl)-2,3,4,5-tetrahydrobenzo[f][1,4]oxazepine (44). NaBH(OAc)$_3$ (323 mg, 1.52 mmol) was added to a solution of **72** (300 mg, 1.02 mmol) and nicotinaldehyde (96 μL, 1.02 mmol) in dichloroethane

(20 mL) at rt. The reaction mixture was aged at rt for 12 h before adding DCM (75 mL) and washing with saturated aqueous NaHCO$_3$ and brine. The solution was dried over MgSO$_4$, filtered, and concentrated in vacuo to provide an orange oil. Purification by flash chromatography on silica gel eluting with 2% MeOH/DCM provided a colorless oil that was dissolved in ether, and 1 M HCl in ether (1.5 mL) was added to provide the title compound as a white solid (288 mg, 67%). ^{1}H NMR (D$_2$O) δ 2.17 (s, 3H), 3.67 (m, 2H), 4.31 (br s, 2H), 4.37 (s, 2H), 4.61 (s, 2H), 7.09 (br s, 1H), 7.35 (m, 4H), 7.71 (dd, J = 6.3 and 2.8 Hz, 1H), 7.90 (dd, J = 6.3 and 2.4 Hz, 1H), 8.06 (dd, J = 8.0 and 5.7 Hz, 1H), 8.61 (br d, J = 8.2 Hz, 1H), 8.83 (d, J = 5.6 Hz, 1H), 8.89 (s, 1H). ESIMS m/z (rel intensity) 387.1 ([M + H], 100).

7-(Benzo[*b*]thiophen-3-yl)-9-chloro-4-(pyridin-3-ylmethyl)-2,3,4,5-tetrahydrobenzo[*f*][1,4]oxazepine (45). Following the general reductive amination procedure using **79** and nicotinaldehyde provided the title compound as a white solid in 45% yield. ^{1}H NMR (CDCl$_3$) δ 3.20 (m, 2H), 3.74 (s, 2H), 3.91 (s, 2H), 4.24 (m, 2H), 7.10 (d, J = 2.2 Hz, 1H), 7.29 (dd, J = 7.7 and 4.8 Hz, 1H), 7.37 (s, 1H), 7.42 (m, 2H), 7.55 (d, J = 2.0 Hz, 1H), 7.74 (br d, J = 8.1 Hz, 1H), 7.85 (m, 2H), 7.91 (m, 1H), 8.54 (dd, J = 4.7 and 1.3 Hz, 1H), 8.56 (d, J = 1.7 Hz, 1H). ESIMS m/z (rel intensity) 407.1 ([M + H], 100).

8-(Benzo[*b*]thiophen-3-yl)-2-(pyridin-3-ylmethyl)-2,3,4,5-tetrahydro-1*H*-benzo[*c*]azepine (46). Following the general reductive amination procedure using **83** and nicotinaldehyde provided the title compound as a white solid in 44% yield. ^{1}H NMR (CDCl$_3$) δ 1.79 (m, 2H), 3.00 (m, 2H), 3.12 (m, 2H), 3.61 (s, 2H), 3.91 (m, 2H), 7.14 (d, J = 1.8 Hz, 1H), 7.29 (m, 2H), 7.42 (m, 3H), 7.50 (s, 1H), 7.69 (dt, J = 7.8 and 2.0 Hz, 1H), 7.86 (m, 1H), 7.98 (m, 1H), 8.45 (m, 2H). ESIMS m/z (rel intensity) 371.2 ([M + H], 100).

7-(Benzo[*b*]thiophen-3-yl)-4-(pyridin-3-ylmethyl)-2,3,4,5-tetrahydro-1*H*-benzo[*e*][1,4]diazepine (47). Following the general reductive amination procedure using **85** and nicotinaldehyde provided the title compound as a white solid in 53% yield. ^{1}H NMR (CD$_3$CN) δ 3.45 (s, 4H), 4.46 (s, 2H), 4.58 (s, 2H), 7.06 (d, J = 8.2 Hz, 1H), 7.44 (m, 1H), 7.47 (m, 2H), 7.52 (s, 1H), 7.55 (dd, J = 8.2 and 2.0 Hz, 1H), 7.93 (m, 1H), 7.95 (m, 1H), 8.00 (m, 1H), 8.49 (d, J = 7.8 Hz, 1H), 8.84 (br s, 1H), 8.94 (br s, 1H). ESIMS m/z (rel intensity) 372.1 ([M + H], 100).

7-(Benzo[*b*]thiophen-3-yl)-1-methyl-4-(pyridin-3-ylmethyl)-2,3,4,5-tetrahydro-1*H*-benzo[*e*][1,4]diazepine (48). To a mixture of **47** (54 mg, 0.111 mmol), formaldehyde (0.111 mmol), and 3 Å molecular sieves in MeOH at rt was added NaCNBH$_3$ (10 mg, 0.167 mmol). The reaction mixture was stirred at rt for 48 h, concentrated in vacuo, and purified by flash chromatography on silica gel eluting with 0−10% MeOH/DCM to provide the title compound as a white solid (14.2 mg, 33%). ^{1}H NMR (CD$_3$CN) δ 2.91 (m, 2H), 2.92 (s, 3H), 3.05 (m, 2H), 3.65 (s, 2H), 3.78 (s, 2H), 7.05 (d, J = 8.2 Hz, 1H), 7.18 (d, J = 2.0 Hz, 1H), 7.30 (ddd, J = 7.8, 4.7, and 0.8 Hz, 1H), 7.48−7.38 (m, 3 H), 7.44 (s, 1H), 7.72 (m, 1H), 7.90 (m, 1H), 7.96 (m, 1H), 8.46 (dd, J = 4.9 and 1.8 Hz, 1H), 8.50 (m, 1H). ESIMS m/z (rel intensity) 386.2 ([M + H], 100).

7-(Benzo[*b*]thiophen-3-yl)-9-methoxy-4-(pyridin-3-ylmethyl)-4,5-dihydrobenzo[*f*][1,4]oxazepin-3(2*H*)-one (49). NaBH(OAc)$_3$ (824 mg, 3.89 mmol) was added to a solution of **87** (960 mg, 2.59 mmol) and pyridin-3-ylmethanamine (290 μL, 2.35 mmol) in dichloroethane (40 mL) at rt. The reaction mixture was stirred at rt for 2 h, at which point LCMS indicated that the reductive amination was complete. The reaction mixture was heated at reflux for 4.5 h, cooled to rt, diluted with EtOAc (100 mL), and washed with water (75 mL), saturated aqueous NaHCO$_3$, and brine, and dried over MgSO$_4$, filtered, and concentrated in vacuo to provide a brown oil. Purification by flash chromatography on silica gel eluting with 2% MeOH/DCM provided the title compound as an off-white solid (786 mg, 73%). ^{1}H NMR (CDCl$_3$) δ 3.89 (s, 3H), 4.46 (s, 2H), 4.78 (s, 2H), 4.81 (s, 2H), 6.67 (d, J = 2.0 Hz, 1H), 7.07 (d, J = 2.0 Hz, 1H), 7.22 (s, 1H), 7.24−7.20 (m, 1H), 7.36 (m, 2H), 7.59 (dt, J = 7.8 and 2.0 Hz, 1H), 7.68 (m, 1H), 7.87 (m, 1H), 8.53 (dd, J = 4.7 and 1.6 Hz, 1H), 8.55 (d, J = 2.0 Hz, 1H). ESIMS m/z (rel intensity) 417.1 ([M + H], 100).

7-(Benzo[*b*]thiophen-3-yl)-9-methoxy-4-(pyridin-3-ylmethyl)-3,4-dihydrobenzo[*f*][1,4]oxazepin-5(2*H*)-one (50). NaH (60% in

mineral oil) (4.5 mg, 0.117 mmol) was added to a solution of **90** (19 mg, 0.058 mmol) in anhydrous THF (1 mL) at rt followed by the addition of 3-(bromomethyl)pyridine hydrobromide (15 mg, 0.058 mmol). The reaction mixture was stirred at rt for 12 h, quenched with water (1 mL), and extracted with EtOAc (3 × 2 mL). The organics were combined, dried over Na$_2$SO$_4$, filtered, and concentrated in vacuo. Purification by flash chromatography on silica gel eluting with 0−10% MeOH/DCM provided the title compound as a white solid (6.9 mg, 28%). ^{1}H NMR (CDCl$_3$) δ 3.56 (t, J = 5.5 Hz, 2H), 3.89 (s, 3H), 4.26 (t, J = 5.5 Hz, 2H), 4.82 (s, 2H), 7.34 (dd, J = 7.9 and 4.9 Hz, 1H), 7.36 (d, J = 2.4 Hz, 1H), 7.48−7.42 (m, 3H), 7.63 (s, 1H), 7.76 (m, 1H), 7.99 (m, 2H), 8.51 (dd, J = 4.6 and 1.5 Hz, 1H), 8.60 (d, J = 1.8 Hz, 1H). ESIMS m/z (rel intensity) 417.1 ([M + H], 100).

4-((7-(Benzo[*b*]thiophen-3-yl)-9-chloro-2,3-dihydrobenzo[*f*]-[1,4]oxazepin-4(5*H*)-yl)methyl)pyridin-2(1*H*)-one (51). Following the general reductive amination procedure using **79** and 2-hydroxyisonicotinaldehyde provided the title compound as a white solid in 92% yield. ^{1}H NMR (DMSO-*d*$_6$) δ 2.58 (br s, 2H), 3.77 (br s, 4H), 4.33 (br s, 2H), 6.26 (d, J = 6.7 Hz, 1H), 6.41 (br s, 1H), 7.53−7.43 (m, 4H), 7.72 (br s, 1H), 7.89 (s, 1H), 7.91 (m, 1H), 8.09 (d, J = 7.4 Hz, 1H). ESIMS m/z (rel intensity) 423.1 ([M + H], 100).

4-((9-Chloro-7-(5-fluoro-1*H*-indol-1-yl)-2,3-dihydrobenzo[*f*]-[1,4]oxazepin-4(5*H*)-yl)methyl)pyridin-2(1*H*)-one (52). Following the general reductive amination procedure, **95** (13.15 g, 41.5 mmol) and 2-hydroxyisonicotinaldehyde (5.62 g, 45.7 mmol) provided the title compound as an off-white solid (10.0 g, 57%). ^{1}H NMR (CDCl$_3$) δ 3.20 (m, 2H), 3.60 (s, 2H), 3.90 (s, 2H), 4.23 (m, 2H), 6.43 (dd, J = 6.7 and 1.2 Hz, 1H), 6.56 (br s, 1H), 6.62 (dd, J = 3.5 and 0.8 Hz, 1H), 7.01 (td, J = 9.1 and 2.5 Hz, 1H), 7.07 (d, J = 2.8 Hz, 1H), 7.29 (m, 2H), 7.34 (d, J = 6.7 Hz, 1H), 7.40 (dd, J = 9.0 and 4.3 Hz, 1H), 7.45 (d, J = 2.7 Hz, 1H). ESIMS m/z (rel intensity) 424.2 ([M + H], 100).

(*R*)-4-((7-(Benzo[*b*]thiophen-3-yl)-9-chloro-3-methyl-2,3-dihydrobenzo[*f*][1,4]oxazepin-4(5*H*)-yl)methyl)pyridin-2(1*H*)-one (53). Following the general reductive amination procedure, **94** (100 mg, 0.303 mmol) and 2-hydroxyisonicotinaldehyde (37.3 mg, 0.303 mmol) provided the title compound as a white solid (43.2 mg, 33%). ^{1}H NMR (CDCl$_3$) δ 1.22 (d, J = 7.0 Hz, 3H), 3.20 (m, 1H), 3.41 (d, J = 15.7 Hz, 1H), 3.54 (d, J = 15.7 Hz, 1H), 3.67 (d, J = 15.7 Hz, 1H), 3.96 (dd, J = 12.9 and 6.3 Hz, 1H), 4.16 (m, 2H), 6.30 (d, J = 6.7 Hz, 1H), 6.47 (s, 1H), 6.99 (d, J = 2.0 Hz, 1H), 7.23 (d, J = 6.7 Hz, 1H), 7.34−7.28 (m, 3H), 7.44 (d, J = 2.4 Hz, 1H), 7.73 (d, J = 7.4 Hz, 1H), 7.79 (d, J = 7.4 Hz, 1H). ESIMS m/z (rel intensity) 437.0 ([M + H], 100).

(*R*)-4-((9-Chloro-7-(5-fluoro-1*H*-indol-1-yl)-3-methyl-2,3-dihydrobenzo[*f*][1,4]oxazepin-4(5*H*)-yl)methyl)pyridin-2(1*H*)-one (54). Following the general reductive amination procedure, **96** (10.53 g, 31.8 mmol) and 2-hydroxyisonicotinaldehyde (4.31 g, 35.0 mmol) provided the title compound as a white solid (9.45 g, 68%). ^{1}H NMR (CDCl$_3$) δ 1.36 (d, J = 6.7 Hz, 3H), 3.36 (m, 1H), 3.55 (d, J = 15.3 Hz, 1H), 3.68 (d, J = 15.3 Hz, 1H), 3.79 (d, J = 15.8 Hz, 1H), 4.08 (dd, J = 12.8 and 6.4 Hz, 1H), 4.28 (m, 2H), 6.43 (br s, 1H), 6.54 (s, 1H), 6.61 (dd, J = 3.3 and 0.6 Hz, 1H), 7.01 (td, J = 9.0 and 2.5 Hz, 1H), 7.03 (s, 1H), 7.28 (m, 2H), 7.33 (d, J = 6.7 Hz, 1H), 7.39 (dd, J = 9.0 and 4.3 Hz, 1H), 7.45 (d, J = 2.5 Hz, 1H). ESIMS m/z (rel intensity) 438.2 ([M + H], 100).

■ ASSOCIATED CONTENT

ⓈSupporting Information

Experimental procedures describing the preparation of intermediates and protocols for the in vitro assays and phagocytosis assay (PDF, CSV). The Supporting Information is available free of charge on the ACS Publications website at DOI: 10.1021/acs.jmedchem.5b00567.

■ AUTHOR INFORMATION

Corresponding Author

*Phone: (650) 430-3814. E-mail: fox11.brian@gmail.com.

Author Contributions

The manuscript was written through contributions of all authors. All authors have given approval to the final version of the manuscript.

Notes

The authors declare no competing financial interest.

■ ABBREVIATIONS USED

AD, Alzheimer's disease; Aβ, amyloid-beta; IL-1β, interleukin-1β; IL-6, interleukin-6; TNF-α, tumor necrosis factor-α; IL-8, interleukin-8; MIP-1α, macrophage inflammatory protein-1α; MCP-1, monocyte chemoattractant peptide-1; PGE$_2$, prostaglandin E$_2$; LPS, lipopolysaccharide; PK, pharmacokinetic

■ REFERENCES

(1) Braak, H.; Braak, E. Frequency of stages of Alzheimer-related lesions in different age categories. *Neurobiol. Aging* **1997**, *18*, 351−357.

(2) Rogers, J.; Strohmeyer, R.; Kovelowski, C. J.; Li, R. Microglia and inflammatory mechanisms in the clearance of amyloid beta peptide. *Glia* **2002**, *40*, 260−269.

(3) Shie, F.-S.; Breyer, R. M.; Montine, T. J. Microglia lacking E prostanoid receptor subtype 2 have enhanced Aβ phagocytosis yet lack Aβ-activated neurotoxicity. *Am. J. Pathol.* **2005**, *166*, 1163−1172.

(4) Simard, A. R.; Soulet, D.; Gowing, G.; Julien, J.-P.; Rivest, S. Bone marrow-derived microglia play a critical role in restricting senile plaque formation in Alzheimer's disease. *Neuron* **2006**, *49*, 489−502.

(5) Stalder, M.; Phinney, A.; Probst, A.; Sommer, B.; Staufenbiel, M.; Jucker, M. Association of microglia with amyloid plaques in brains of APP23 transgenic mice. *Am. J. Pathol.* **1999**, *154*, 1673−1684.

(6) Frautschy, S. A.; Yang, F.; Irrizarry, M.; Hyman, B.; Saido, T. C.; Hsiao, K.; Cole, G. M. Microglial response to amyloid plaques in APPsw transgenic mice. *Am. J. Pathol.* **1998**, *152*, 307−317.

(7) Perlmutter, L. S.; Scott, S. A.; Barron, E.; Chui, H. C. MHC class II-positive microglia in human brain: association with Alzheimer lesions. *J. Neurosci. Res.* **1992**, *33*, 549−558.

(8) Dickson, D. W.; Farlo, J.; Davies, P.; Crystal, H.; Fuld, P.; Yen, S-H. C. A double-labeling immunohistochemical study of senile plaques. *Am. J. Pathol.* **1988**, *132*, 86−101.

(9) Itagaki, S.; McGreer, P. L.; Akiyama, H.; Zhu, S.; Selkoe, D. Relationship of microglia and astrocytes to amyloid deposits of Alzheimer disease. *J. Neuroimmunol.* **1989**, *24*, 173−182.

(10) Sheng, J. G.; Mrak, R. E.; Griffin, W. S. T. Neuritic plaque evolution in Alzheimer's disease is accompanied by transition of activated microglia from primed to enlarged to phagocytic forms. *Acta Neuropathol.* **1997**, *94*, 1−5.

(11) Malm, T. N.; Koistinaho, M.; Pärepalo, M.; Vatanen, T.; Ooka, A.; Karlsson, S.; Koistinaho, J. Bone-marrow-derived cells contribute to the recruitment of microglial cells in response to beta-amyloid deposition in APP/PS1 double transgenic Alzheimer mice. *Neurobiol. Dis.* **2005**, *18*, 134−142.

(12) Kalaria, R. N.; Cohen, D. L.; Premkumar, D. R. D. Cellular aspects of the inflammatory response in Alzheimer's disease. *Neurodegeneration* **1996**, *5*, 497−503.

(13) Bacskai, B. J.; Kajdasz, S. T.; Christie, R. H.; Carter, C.; Games, D.; Seubert, P.; Schenk, D.; Hyman, B. T. Imaging of amyloid-β deposits in brains of living mice permits direct activation of clearance of plaques with immunotherapy. *Nature Med.* **2001**, *7*, 369−372.

(14) Liu, Y.; Walter, S.; Stagi, M.; Cherny, D.; Letiembre, M.; Schulz-Schaeffer, W.; Heine, H.; Penke, B.; Neumann, H.; Fassbender, K. LPS receptor (CD14): a receptor for phagocytosis of Alzheimer's amyloid peptide. *Brain* **2005**, *128*, 1778−1789.

(15) Nicoll, J. A. R.; Wilkinson, D.; Holmes, C.; Steart, P.; Markham, H.; Weller, R. O. Neuropathology of human Alzheimer disease after immunization with amyloid-β peptide: a case report. *Nature Med.* **2003**, *9*, 448−452.

(16) Kim, S. U.; de Vellis, J. Microglia in health and disease. *J. Neurosci. Res.* **2005**, *81*, 302−313.

(17) McDonald, D. R.; Brunden, K. R.; Landreth, G. E. Amyloid fibrils activate tyrosine kinase-dependent signaling and superoxide production in microglia. *J. Neurosci.* **1997**, *17*, 2284−2294.

(18) Lue, L. F.; Walker, D. G.; Rogers, J. Modeling microglial activation in Alzheimer's disease with human postmortem microglial cultures. *Neurobiol. Aging* **2001**, *22*, 945−956.

(19) Floden, A. M.; Li, S.; Combs, C. K. β-Amyloid-stimulated microglia induce neuron death via synergistic stimulation of tumor necrosis factor α and NMDA receptors. *J. Neurosci.* **2005**, *25*, 2566−2575.

(20) Hickman, S. E.; Allison, E. K.; El Khoury, J. Microglial dysfunction and defective β-amyloid clearance pathways in aging Alzheimer's disease mice. *J. Neurosci.* **2008**, *28*, 8354−8360.

(21) Krabbe, G.; Halle, A.; Matyash, V.; Rinnenthal, J. L.; Eom, G. D.; Bernhardt, U.; Miller, K. R.; Prokop, S.; Kettenmann, H.; Heppner, F. L. Functional impairment of microglia coincides with beta-amyloid deposition in mice with Alzheimer-like pathology. *PLoS One* **2013**, *8*, e60921.

(22) Fiala, M.; Lin, J.; Ringman, J.; Kermani-Arab, V.; Tsao, G.; Patel, A.; Lossinsky, A. S.; Graves, M. C.; Gustavson, A.; Sayre, J.; Sofroni, E.; Suarez, T.; Chiappelli, F.; Bernard, G. Ineffective phagocytosis of amyloid-beta by macrophages of Alzheimer's disease patients. *J. Alzheimer's Dis.* **2005**, *7*, 221−232.

(23) Mawuenyega, K. G.; Sigurdson, W.; Ovod, V.; Munsell, L.; Kasten, T.; Morris, J. C.; Yarasheki, K. E.; Bateman, R. J. Decreased clearance of CNS β-amyloid in Alzheimer's disease. *Science* **2010**, *330*, 1774.

(24) Akiyama, H.; Barger, S.; Barnum, S.; Bradt, B.; Bauer, J.; Cole, G. M.; Cooper, N. R.; Eikelenboom, P.; Emmerling, M.; Fiebich, B. L.; Finch, C. E.; Frautschy, S.; Griffin, W. S. T.; Hampel, H.; Hull, M.; Landreth, G.; Lue, L.-F.; Mrak, R.; Mackenzie, I. R.; McGreer, P. L.; O'Banion, M. K.; Pachter, J.; Pasinetti, G.; Plata-Salaman, C.; Rogers, J.; Rydel, R.; Shen, Y.; Streit, W.; Strohmeyer, R.; Tooyoma, I.; Van Muiswinkel, F. L.; Veerhius, R.; Walker, D.; Webster, S.; Wegrzyniak, B.; Wenk, G.; Wyss-Coray, T. Inflammation and Alzheimer's disease. *Neurobiol. Aging* **2000**, *21*, 383−421.

(25) Aronoff, D. M.; Canetti, C.; Peters-Golden, M. Prostaglandin E$_2$ inhibits alveolar macrophage phagocytosis through an E-prostanoid 2 receptor-mediated increase in intracellular cyclic AMP. *J. Immunol.* **2004**, *173*, 559−565.

(26) Montine, T. J.; Sidell, K. R.; Crews, B. C.; Markesbery, W. R.; Marnett, L. J.; Roberts, L. J., II; Morrow, J. D. Elevated CSF prostaglandin E$_2$ levels in patients with probable AD. *Neurology* **1999**, *53*, 1495−1498.

(27) Breyer, R. M.; Bagdassarian, C. K.; Myers, S. A.; Breyer, M. D. Prostanoid receptors: subtypes and signaling. *Annu. Rev. Pharmacol. Toxicol.* **2001**, *41*, 661−690.

(28) Liang, X.; Wang, Q.; Hand, T.; Wu, L.; Breyer, R. M.; Montine, T. J.; Andreasson, K. Deletion of the prostaglandin E2 EP2 receptor reduces oxidative damage and amyloid burden in a model of Alzheimer's Disease. *J. Neurosci.* **2005**, *25*, 10180−10187.

(29) Keene, C. D.; Chang, R. C.; Lopez-Yglesias, A. H.; Shalloway, B. R.; Sokal, I.; Li, X.; Reed, P. J.; Keene, L. M.; Montine, K. S.; Breyer, R. M.; Rockhill, J. K.; Montine, T. J. Suppressed accumulation of cerebral amyloid β peptides in aged transgenic Alzheimer's disease mice by transplantation with wild-type or prostaglandin E$_2$ receptor subtype 2-null bone marrow. *Am. J. Pathol.* **2010**, *177*, 346−354.

(30) Johansson, J. U.; Pradhan, S.; Lokteva, L. A.; Woodling, N. S.; Ko, N.; Brown, H. D.; Wang, Q.; Loh, C.; Cekanaviciute, E.; Buckwalter, M.; Manning-Bog, A. B.; Andreasson, K. I. Suppression of inflammation with conditional deletion of the prostanoid E$_2$ EP2 receptor in macrophages and brain microglia. *J. Neurosci.* **2013**, *33*, 16016−16032.

(31) Montine, T. J.; Milatovic, D.; Gupta, R. C.; Valyi-Nagy, T.; Morrow, J. D.; Breyer, R. M. Neuronal oxidative damage from activated innate immunity is EP$_2$ receptor-dependent. *J. Neurochem.* **2002**, *83*, 463−470.

(32) Shie, F.-S.; Montine, K. S.; Breyer, R. M.; Montine, T. J. Microglial EP2 is critical to neurotoxicity from activated cerebral innate immunity. *Glia* **2005**, *52*, 70−77.

(33) Johansson, J. U.; Woodling, N. S.; Wang, Q.; Panchal, M.; Liang, X.; Trueba-Saiz, A.; Brown, H. D.; Mhatre, S. D.; Loui, T.; Andreasson, K. I. Prostaglandin signaling suppresses beneficial microglial function in Alzheimer's disease models. *J. Clin. Invest.* **2015**, *125*, 350−364.

(34) Ganesh, T. Prostanoid receptor EP2 as a therapeutic target. *J. Med. Chem.* **2014**, 4454−4465.

(35) Forselles, K. J.; Root, J.; Clarke, T.; Davey, D.; Aughton, K.; Dack, K.; Pullen, N. In vitro and in vivo characterization of PF-04418948, a novel, potent and selective prostaglandin EP$_2$ receptor antagonist. *Br. J. Pharmacol.* **2011**, *164*, 1847−1856.

(36) Birrell, M. A.; Maher, S. A.; Buckley, J.; Dale, N.; Bonvini, S.; Raemdonck, K.; Pullen, N.; Giembycz, M. A.; Belvisi, M. G. Selectivity profiling of the novel EP$_2$ receptor antagonist, PF-04418948, in functional bioassay systems: atypical affinity at the guinea pig EP$_2$ receptor. *Br. J. Pharmacol.* **2013**, *168*, 129−138.

(37) Jiang, J.; Ganesh, T.; Du, Y.; Quan, Y.; Serrano, G.; Qui, M.; Speigel, I.; Rojas, A.; Lelutiu, N.; Dingeldine, R. Small molecule antagonist reveals seizure-induced mediation of neuronal injury by prostaglandin E2 receptor subtype EP2. *Proc. Natl. Acad. Sci. U. S. A.* **2012**, *109*, 3149−3154.

(38) Jiang, J.; Quan, Y.; Ganesh, T.; Pouliot, W. A.; Dudek, F. E.; Dingledine, R. Inhibition of the prostaglandin receptor EP2 following status epilepticus reduces delayed mortality and brain inflammation. *Proc. Natl. Acad. Sci. U. S. A.* **2013**, *110*, 3591−3596.

(39) Ganesh, T.; Jiang, J.; Shashidharamurthy, R.; Dingeldine, R. Discovery and characterization of carbamothioylacrylamides as EP2 selective antagonists. *ACS Med. Chem. Lett.* **2013**, *4*, 616−621.

(40) Ganesh, T.; Jiang, J.; Dingeldine, R. Development of second generation EP2 antagonists with high selectivity. *Eur. J. Med. Chem.* **2014**, *82*, 521−535.

(41) Ganesh, T.; Jiang, J.; Yang, M.-S.; Dingeldine, R. Lead optimization studies of cinnamic amide EP2 antagonists. *J. Med. Chem.* **2014**, *57*, 4173−4184.

(42) Rendic, S.; Di Carlo, F. J. Human cytochrome P450 enzymes: a status report summarizing their reactions, substrates, inducers, and inhibitors. *Drug Metab. Rev.* **1997**, *29*, 413−580.

(43) Riley, R. J.; Parker, A. J.; Trigg, S.; Manners, C. N. Development of a generalized, quantitative physicochemical model of CYP3A4 inhibition for use in early drug discovery. *Pharm. Res.* **2001**, *18*, 652−655.

(44) Caggiano, A. O.; Kraig, R. P. Prostaglandin E receptor subtypes in cultured rat microglia and their role in reducing lipopolysaccharide-induced interleukin-1β production. *J. Neurochem.* **1999**, *72*, 565−575.

(45) Hsiao, K.; Chapman, P.; Nilsen, S.; Eckman, C.; Harigaya, Y.; Younkin, S.; Yang, F.; Cole, G. Correlative memory deficits, Aβ elevation, and amyloid plaques in transgenic mice. *Science* **1996**, *274*, 99−102.

(46) Barder, T. E.; Walker, S. D.; Martinelli, J. R.; Buchwald, S. L. Catalysts for Suzuki−Miyaura coupling processes: scope and studies of the effect of ligand structure. *J. Am. Chem. Soc.* **2005**, *127*, 4685−4696.

(47) Node, M.; Kumar, K.; Nishide, K.; Ohsugi, S.-I.; Miyamoto, T. Odorless substitutes for foul-smelling thiols: syntheses and applications. *Tetrahedron Lett.* **2001**, *42*, 9207−9210.

(48) Krow, G. R. Nitrogen insertion reactions of bridged bicyclic ketones. Regioselective lactam formation. *Tetrahedron* **1981**, *37*, 1283−1307.

(49) Antilla, J. C.; Klapars, A.; Buchwald, S. L. The copper-catalyzed N-arylation of indoles. *J. Am. Chem. Soc.* **2002**, *124*, 11684−11688.

(50) Liu, L.; Frohn, M.; Xi, N.; Dominguez, C.; Hungate, R.; Reider, P. J. A soluble base for the copper-catalyzed imidazole arylations with aryl halides. *J. Org. Chem.* **2005**, *70*, 10135−10138.